

0.092, and 0.154 Å (molecule 2). Peripheral C(3,4) atom deviations vary between 0.00 and 0.50 Å, depending on whether the pyrrolidine ring has 2-fold or "envelope" symmetry.

In the absence of a substantial array of complexes of the type $L_{(2)}CuBr_2CuL_{(2)}$, for comparative discussion of the Cu_2Br_2 moiety, a useful base line structural type is that of $[Cu(NH_3)_4](CuBr)_2$.¹¹ This, like its chloride analogue, crystallizes in space group $I4/mmm$ and contains infinite $-CuBr_2CuBr_2CuBr_2Cu-$ chains, with the copper atoms located on Wyckoff position d at $(0, 1/2, 1/4)$ etc. with symmetry $4m2$ and separated from their congeners within the polymer at $(0, 1/2, 3/4)$ etc. by $c/2$ ($=2.857$ (4) (bromide), 2.734 (4) Å (chloride)), while the bromide at $(x, 1/2, 0)$ (Wyckoff j) is separated by $2x = 0.3968$ (0.3774 (chloride) $a = 4.12$ (3.85 Å chloride)). These latter values are slightly greater than the usual van der Waals estimates of ~ 3.9 and 3.6 Å, respectively,¹² while the former may be compared with the interatomic separation in the metal of 2.56 Å.¹³ $Cu\cdots Cu$ in the present complex is nearer the value observed in the metal, being 2.697 (2) Å, while $Br\cdots Br$, 4.013 Å, is also shorter than in the anion polymer. The shortening of both of these distances simultaneously in the present complex may be attributed to relatively weak copper-sulfur bonding, effectively diminishing the coordination number of the copper atom. The copper-sulfur distance in copper(I) carbodithioate

complexes has only been established for the tetrameric $[Cu(S_2CNEt_2)]_4$ species¹⁴ in which it ranges from 2.246 (7) to 2.290 (6) Å. Values obtained for a variety of similar but not truly parallel interspecies interactions such as the trigonal $S_2\cdots CuBr$ array in $(t-BuNC)_4Mo(\pm-t-BuS)_2CuBr$ (2.233 (3)– 2.244 (3) Å¹⁵), $[[\text{piperidine } N\text{-oxide}(1-)]_2Mo(\pm-S)_2Cu(\pm-Cl)]_2$ (2.266 (1) Å⁴ (tetrahedral Cu), $[Cu(S_2CNC_5H_{10})_2](CuBr)_4$, (2.3163 (9) Å), and $[Cu(S_2CNC_5H_{10})_2](CuBr)_6$ (2.284 (4), 2.305 (2), 2.476 (3) Å)¹⁶ all tend to indicate the norm for a copper(I)-sulfur interaction in the context of trigonal or tetrahedral environments to be considerably less than the present values that range from 2.390 (2) to 2.431 (2) Å. The weakness of this interaction is corroborated by the relatively small perturbations noted above on the geometry of the $Co(dtc)_3$ molecule. Accordingly, the geometry of the Cu_2Br_2 species may perhaps be regarded as more akin to that of a matrix-isolated dimer.

Acknowledgment. We gratefully acknowledge support of this work by a grant from the Australian Research Grants Scheme.

Registry No. $(Co(dtc)_3)CuBr_2Cu(Co(dtc)_3)$, 93984-80-6.

Supplementary Material Available: Listings of thermal parameters, hydrogen parameters, least-squares planes, ligand geometries, and observed and calculated structure factor amplitudes (23 pages). Ordering information is given on any current masthead page.

- (11) J. A. Baglia and P. A. Vaughan, *J. Inorg. Nucl. Chem.*, **32**, 803 (1970).
 (12) L. Pauling, "The Nature of the Chemical Bond", 3rd ed., Cornell University Press, Ithaca, NY, 1960, p 260.
 (13) A. F. Wells, "Structural Inorganic Chemistry", 4th ed., Pergamon Press, Oxford, 1975, p 1023.

- (14) R. Hesse, *Ark. Kemi*, **20**, 481 (1963).
 (15) N. C. Payne, N. Okura, and S. Otsuka, *J. Am. Chem. Soc.*, **105**, 245 (1983).
 (16) R. M. Golding, A. D. Rae, B. J. Ralph, and L. Sulligoi, *Inorg. Chem.*, **13**, 2499 (1974).

Contribution from the Department of Chemistry,
 The University of North Carolina, Chapel Hill, North Carolina 27514

Directed, Intramolecular Electron Transfer in Mixed-Valence Dimers

JEFF C. CURTIS,[†] JAMES S. BERNSTEIN,[‡] and THOMAS J. MEYER^{*§}

Received April 11, 1984

One-electron oxidation of the dimers $[(dpte)_2ClRu^{II}(L)Ru^{III}Cl(bpy)]_2^{2+}$ ($dpte = PhSCH_2CH_2SPh$; $bpy = 2,2'$ -bipyridine; $L = 4,4'$ -bipyridine ($4,4'$ -bpy), *trans*-1,2-bis(4-pyridyl)ethylene (bpe), 1,2-bis(4-pyridyl)ethane (bpa)) gives the corresponding mixed-valence dimers $[(dpte)_2ClRu^{II}(L)Ru^{III}Cl(bpy)]_2^{3+}$. In the mixed-valence dimers, $Ru(II) \rightarrow Ru(III)$ intervalence-transfer (IT) bands are observed. Photolysis into either the $\pi^*(bpy) \leftarrow d\pi(Ru^{II}Cl(bpy)_2)$ chromophore for the $Ru(II)$ - $Ru(II)$ dimers or the $\pi^*(L) \leftarrow d\pi(Ru^{II}Cl(dpte)_2)$ chromophore for the mixed-valence dimers results in population of the bpy-based, ³MLCT excited state ($-Ru^{III}Cl(bpy^-)(bpy)^*$) as shown by comparisons between room-temperature emission and low-temperature (220–280 K) transient absorption properties of the dimers and the related monomers $[(bpy)_2ClRu(L)]^+$. The appearance of the ³MLCT-bpy-based emission in the mixed-valence dimers shows that following $\pi^*(L) \leftarrow d\pi(Ru^{II}Cl(dpte)_2)$ excitation, ligand to ligand electron transfer, $[(dpte)_2ClRu^{III}(L^-)Ru^{III}Cl(bpy)_2]^{3+*} \rightarrow [(dpte)_2ClRu^{III}(L)Ru^{III}Cl(bpy^-)(bpy)]^{3+*}$, occurs and is competitive with excited-state nonradiative decay by ligand to metal electron transfer, $[(dpte)_2ClRu^{II}(L)Ru^{III}Cl(bpy)_2]^{3+*} \leftarrow [(dpte)_2ClRu^{III}(L^-)Ru^{III}Cl(bpy)_2]^{3+*} \rightarrow [(dpte)_2ClRu^{II}(L)Ru^{III}Cl(bpy)_2]^{3+}$. Because of the relatively long lifetime of the ³MLCT-bpy state, it is not possible to observe relaxation of the high-energy, mixed-valence isomer to the ground state, $[(dpte)_2ClRu^{II}(L)Ru^{III}Cl(bpy)_2]^{3+} \rightarrow [(dpte)_2ClRu^{III}(L)Ru^{III}Cl(bpy)_2]^{3+}$, following nonradiative decay of ³MLCT-bpy. For the pentaammine $Ru(II)$ dimers $[(NH_3)_5Ru^{II}(L)Ru^{III}Cl(bpy)]_2^{3+}$ ($L = bpe, 4,4'$ -bpy), excitation into the $\pi^*(bpy) \leftarrow d\pi(Ru^{II})$ chromophore does not lead to emission or transient decay from the ³MLCT-bpy excited state apparently because of intramolecular energy transfer to lower lying, relatively short-lived $(NH_3)_5Ru^{III}(L^-)$ -based MLCT states. The ³MLCT-bpy excited state is also not observed following $\pi^*(bpy) \leftarrow d\pi(Ru^{II})$ excitation in the mixed-valence dimers $[(NH_3)_5Ru^{III}(L)Ru^{II}Cl(bpy)]_2^{4+}$ ($L = 4,4'$ -bpy, bpe) either because of intramolecular quenching by $Ru(III)$ or perhaps because of population of short-lived MLCT states based on the bridging ligand, $(NH_3)_5Ru^{III}(L^-)$.

The nature and extent of the interaction between different chromophores in a single molecule or between a chromophore and a potential quencher has been and remains an area of active research in organic photochemistry. Many "bichromophoric"

molecules have been synthesized and investigated from both the photochemical and photophysical points of view.¹ Established processes in such molecules include intramolecularly sensitized emission, photochemistry, and nonradiative decay by intramo-

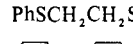
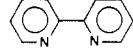
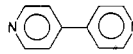
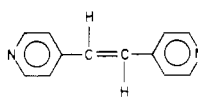
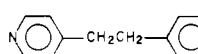
[†] Department of Chemistry, University of San Francisco, San Francisco, CA 94132.

[‡] Burroughs-Wellcome Corporation, Research Triangle Park, NC 27709.

[§] The University of North Carolina.

(1) Getz, D.; Ron, A.; Rubin, M. B.; Speiser, S. *J. Phys. Chem.* **1980**, *84*, 768. (b) Nairn, J. A.; Braun, C. L.; Caluwe, P.; Szwarc, M. *Chem. Phys. Lett.* **1978**, *54*, 469. (c) DeSchryver, F. C.; Boens, N.; Put, J. *Adv. Photochem.* **1977**, *10*, 359. (d) Kosower, E. M. *Acc. Chem. Res.* **1982**, *15*, 259.

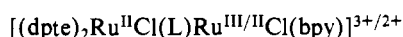
Table I. Ligand Abbreviations and Structures

structure	abbrev	name
	dpte	1,2-bis(diphenylthio)ethane
	bpy	2,2'-bipyridine
	4,4'-bpy	4,4'-bipyridine
	bpe	<i>trans</i> -1,2-bis(4-pyridyl)-ethylene
	bpa	1,2-bis(4-pyridyl)ethane

lecular energy or electron-transfer quenching.

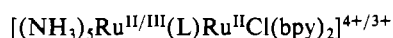
More recently, work has appeared on bichromophoric or chromophore-quencher molecules based on metal complex sites.² The metal-based systems offer a broad range of potentially interesting interactions because of their variable electron contents and redox properties and because of the existence of a variety of different types of electronic excited states; ligand field, charge transfer, intervalence transfer, intraligand, etc.

We report here the results of an investigation on the excited-state properties of a series of bichromophoric ruthenium dimers where the effects of the nature of the bridging ligand, the identity of the lowest lying excited state, and the overall electron content can be varied systematically. Part of this work has appeared as a preliminary communication.³ The dimeric compounds are unsymmetrical and are of two types. The first was based on sites containing either the sulfur chelate 1,2-bis(phenylthio)ethane (dpte, PhSCH₂CH₂SPh) or 2,2'-bipyridine (bpy) as either the Ru(II)-Ru(II) or Ru(II)-Ru(III) mixed-valence dimers:



The structures of the bridging ligands used in the series L = 4,4'-bipyridine (bpy), 1,2-bis(4-pyridyl)ethylene (bpe), 1,2-bis(4-pyridyl)ethane (bpa) are illustrated in Table I. One significant advantage associated with the sulfur-chelated site is the absence of low-lying metal to ligand charge-transfer (MLCT) transitions, which makes the Ru-S site relatively optically transparent.

The second type of dimer was based on the same bridging ligands but utilized pentaammine and bpy sites:



In the pentaammine dimers, the (NH₃)₅Ru^{II}(L)- group is a significant visible chromophore. However, upon oxidation to (NH₃)₅Ru^{III}-, the pentaammine site becomes relatively transparent and a potential oxidative quencher.

Experimental Section

Preparations. Several of the compounds have been previously reported.⁴ The results of elemental analyses both for these compounds and

Table II. Reduction Potentials for the Various Monomeric and Dimeric Compounds in Acetonitrile (0.1 M [N(n-C₄H₉)₄](PF₆)) at 23 ± 2 °C^{a,b}

compd	E _{1/2} (1)	E _{1/2} (2)
[(dpte) ₂ RuCl ₂]	0.62 ± 0.02	
[(dpte) ₂ ClRu(NCCH ₃)](PF ₆)	1.33	
[(dpte) ₂ ClRu(4,4'-bpy)](PF ₆)	1.19	
[(bpy) ₂ ClRu(4,4'-bpy)](PF ₆)	0.79	
[(NH ₃) ₅ Ru(4,4'-bpy)](PF ₆) ₂ ^c	0.43	
[(dpte) ₂ ClRu(4,4'-bpy)RuCl(bpy) ₂](PF ₆) ₂	1.20	0.81
[(NH ₃) ₅ Ru(4,4'-bpy)RuCl(bpy) ₂](PF ₆) ₃	0.82	0.42
[(dpte) ₂ ClRu(bpe)](PF ₆)	1.19	
[(bpy) ₂ ClRu(bpe)](PF ₆)	0.78	
[(NH ₃) ₅ Ru(bpe)](PF ₆) ₂ ^c	0.37	
[(dpte) ₂ ClRu(bpe)RuCl(bpy) ₂](PF ₆) ₂	1.21	0.79
[(NH ₃) ₅ Ru(bpe)RuCl(bpy) ₂](PF ₆) ₃	0.81	0.41
[(dpte) ₂ ClRu(bpa)](PF ₆)	1.18	
[(bpy) ₂ ClRu(bpa)](PF ₆)	0.77	
[(NH ₃) ₅ Ru(bpa)](PF ₆) ₂	0.35	
[(dpte) ₂ ClRu(bpa)RuCl(bpy) ₂](PF ₆) ₂	1.18	0.78
[(NH ₃) ₅ Ru(bpa)RuCl(bpy) ₂](PF ₆) ₃	0.79	0.38

^a E_{1/2} was taken as the midpoint potential between oxidative and reductive current maxima obtained from cyclic voltammetric waves at 200 mV/s. ^b The measurements were made in doubly distilled, anhydrous acetonitrile with 0.1 M TBAH supporting electrolyte on a freshly polished platinum-disk electrode. Potential values are in volts vs. SCE at 23 ± 2 °C in 0.1 M TBAH/acetonitrile. ^c Taken from ref 4a.

for the compounds prepared here for the first time are listed in supplementary tables 1 and 2.

1,2-Bis(phenylthio)ethane (dpte), C₆H₅SCH₂SC₆H₅. The disulfur ligand was initially prepared by a modification of the method of Bell and Bennett.⁵ A 13.5-g (1.23-mol) amount of thiophenol (Aldrich) was stirred at room temperature in 100 mL of absolute ethanol under a blanket of nitrogen in the presence of 3.0 g (1.29 mol) of freshly cut metallic sodium. The reaction was allowed to proceed until all the sodium had dissolved and continued for an additional 1 h. To the solution was added slowly 11.3 g (0.06 mol) of 1,2-dibromoethane (Aldrich), and the mixture was heated at reflux for several hours, cooled, and filtered in order to remove the NaBr precipitate. The yellowish solution was evaporated to dryness on a rotary evaporator and the crude solid dpte recrystallized from absolute ethanol, giving white plates. Yields were on the order of 60% for the final product. In later procedures the ligand was purchased directly from Farifield Chemical Co.

***trans*-Bis(bis(phenylthio)ethane)dichlororuthenium(II), *trans*-[(dpte)₂Ru^{II}Cl₂].** This compound was synthesized according to the method of Chatt.⁶ Ruthenium trichloride (1.5 g, 5.6 mol) was heated at reflux with 3.8 g of the dpte ligand (0.15 mol) in 50 mL of 2-methoxyethanol for 1.5 h. The solution was allowed to cool slowly to room temperature and chilled to 0 °C. The product was collected by filtration as 1.8 g of orange-pink microcrystals (50% yield). The crude product was suitable for further preparations and for purposes of elemental analysis and NMR was purified by dissolving it in a minimum of a 2:1 mixture of methylene chloride and acetone and filtering the solution into 6 volumes of acetone. Alternatively, recrystallization from a 6:1 mixture of methyl ethyl ketone and methylene chloride was also used. Anal. Calcd (obsd): C, 50.06 (50.02); H, 4.24 (4.26); Cl, 10.67 (11.18).

Bis(bis(diphenylthio)ethane)chloro(L)ruthenium Hexafluorophosphate, [(dpte)₂RuCl(L)](PF₆), L = Acetonitrile, 4,4'-Bipyridine, 1,2-Bis(4-pyridyl)ethylene, 1,2-Bis(4-pyridyl)ethane. The same procedure was used for all four compounds, which required heating 0.30 g of *trans*-[(dpte)₂RuCl₂] at reflux in 75 mL of an 80% ethanol-20% water mixture in the presence of a fourfold molar excess of L for approximately 2-3 h. The heating was terminated within 15 min of the point at which the cloudy, orange suspension of the starting material completely dissolved to give the yellow-orange color characteristic of [(dpte)₂RuCl(L)]⁺ since heating past this point increases the number of undesirable side products. The solid was collected by adding 5 mL of aqueous NH₄PF₆ to the still hot reaction mixture, cooling with stirring to room temperature, and removing the ethanol with a rotary evaporator. The resulting solid was dissolved in a minimum volume of acetone and filtered into 10 volumes of stirring anhydrous ether in order to remove excess NH₄PF₆ and

- (2) (a) Sullivan, B. P.; Abruna, H.; Finklea, H. O.; Salmon, D. J.; Nagle, J. K.; Meyer, T. J.; Sprintschnik, H. *Chem. Phys. Lett.* **1978**, *58*, 389-393. (b) Nagle, J. K.; Bernstein, J. S.; Young, R. C.; Meyer, T. J. *Inorg. Chem.* **1981**, *20*, 1760-1764. (c) Westmoreland, T. D.; Le Bozec, H.; Murray, R. W.; Meyer, T. J. *J. Am. Chem. Soc.* **1983**, *105*, 5952-5954. (d) Creutz, C.; Kroger, P.; Matsubara, T.; Netzel, T. L.; Sutin, N. *J. Am. Chem. Soc.* **1979**, *101*, 5442. (e) Petersen, J. D.; Jaske, F. P. *J. Am. Chem. Soc.* **1979**, *101*, 3649. (f) Malin, J. M.; Ryan, D. A.; O'Halloran, T. V. *J. Am. Chem. Soc.* **1978**, *100*, 2097; **1976**, *98*, 6045. (g) Ford, P. C.; Durante, V. A. *J. Am. Chem. Soc.* **1975**, *97*, 6898. (h) Gaswick, D.; Haim, A. *J. Am. Chem. Soc.* **1974**, *96*, 7845. (i) Farr, J. K.; Hulett, L. G.; Lane, R. H.; Hurst, J. K. *J. Am. Chem. Soc.* **1975**, *97*, 2654. (j) Volger, A.; Kunkely, H. *Ber. Bunsenges. Phys. Chem.* **1975**, *79*, 301. (k) Gelroth, J. A.; Figard, J. E.; Petersen, J. D. *J. Am. Chem. Soc.* **1979**, *101*, 3649.
- (3) Curtis, J. C.; Bernstein, J. S.; Schmehl, R. H.; Meyer, T. J. *Chem. Phys. Lett.* **1981**, *81*, 48-52.
- (4) (a) Callahan, R. W. Ph.D. Dissertation, The University of North Carolina, Chapel Hill, NC, 1975. (b) Powers, M. J.; Callahan, R. W.; Salmon, D. J.; Meyer, T. J. *Inorg. Chem.* **1976**, *15*, 894.

(5) Bell, E. V.; Bennett, G. M. *J. Am. Soc.* **1928**, 3189.

(6) Chatt, J.; Leigh, G. J.; Storace, A. P. *J. Chem. Soc. A* **1971**, 1380. See also: Crosby, G. A.; Klassen, D. M. *J. Mol. Spectrosc.* **1968**, *25*, 398.

starting material. The solid was collected by filtration and chromatographed on alumina with use of a mixture of 3:1 benzene/acetonitrile with 1% methanol added. The principal band that elutes first was collected by evaporation, and the resulting solid was dissolved in a minimum volume of acetonitrile and filtered into 10 volumes of stirring ether. The product was collected by filtration, washed with several 15-mL portions of anhydrous ether, and dried in a vacuum desiccator. Analytical and spectral data for the compounds are summarized in supplementary tables 2 and 3 and electrochemical data in Table II. Yields for the final products were typically between 60% and 40%.

$[(dpte)_2Ru^{II}Cl(L)Ru^{III}Cl(bpy)_2](PF_6)_2$, L = 4,4'-bpy, bpe, bpa. The mixed dpte-bpy dimers were synthesized in two different ways.

Method A. This method utilized $[(bpy)_2RuCl(S)]^+$, where S = acetone, as an intermediate.^{7a} In a typical preparation, 0.055 g (0.1 mol) of $[(bpy)_2Ru^{II}Cl_2]$ was stirred at room temperature for 1 h in 30 mL of degassed acetone in the presence of 0.022 g (0.09 mmol) of $AgPF_6$ (Alfa-Ventron). To the resulting solution of the chloro-solvent complex was added 0.05 mmol of the appropriate $[(dpte)_2Ru^{II}Cl](PF_6)$ complex. The mixture was heated at reflux for at least 8 h; reaction times as long as 24 h proved worthwhile in terms of increasing the yield. The solvent volume was reduced to about 4 or 5 mL, and the remaining solution was filtered into 10 volumes of stirring anhydrous ether, which removed the solid $AgCl$ byproduct. The resulting solid was collected by filtration and chromatographed on alumina with 3:1 benzene/acetonitrile and 1% methanol as eluent. The desired dimeric product, $[(dpte)_2ClRu^{II}(L)Ru^{III}Cl(bpy)_2](PF_6)_2$, was obtained as the second band (orange to orange-red), which appeared after a minor yellow band of unreacted $[(dpte)_2Ru^{II}Cl(L)](PF_6)$ was eluted. Generally speaking, several red bands were not eluted, including those containing $[(bpy)_2Ru^{II}Cl(NCCH_3)](PF_6)$ and $[(bpy)_2Ru^{II}Cl_2]$. The dimers decompose slowly (hours) on the column, particularly the bpa-bridged dimer. The volume of the eluted solution was reduced by evaporation and the dimer precipitated by filtering into 10 volumes of stirring ether. Yields were typically on the order of 30–50%. The solids were purified by dissolving them in a small volume (3–5 mL) of acetonitrile, chilling the soln. to 0 °C, and layering in an approximately equal volume of anhydrous ether slowly onto the top of the acetonitrile layer. Over a period of 1 or 2 days these solutions deposited about a 50% yield of analytically pure product.

Method B. In this method the solvent species $[(bpy)_2Ru^{II}(S)Cl]^+$, where S = H_2O , was the reactive intermediate.^{7a} Typically, 0.050 g (0.05 mmol) of the appropriate monomer $[(dpte)_2Ru^{II}Cl(L)](PF_6)$ was heated at reflux with 0.030 g (0.06 mmol) of $[(bpy)_2Ru^{II}Cl_2]$ in 50 mL of 80% ethanol–20% water for 6 h. The crude dimeric product was precipitated by adding 5 mL of a saturated solution of NH_4PF_6 in water and then stripping off the ethanol on a rotary evaporator. The solid was isolated by filtration, dissolved in a small volume (ca. 5 mL) of acetone, and filtered into 10 volumes of stirring anhydrous ether. The resulting precipitate was chromatographed and purified as in method A. This route, although very simple, gave only 20% yields largely because of the formation of mixed chloride-hexafluorophosphate salts in the initial isolation step and the less labile nature of the aquo ligand vs. acetone. Elemental analysis data for the dimers are listed in supplementary table 2.

$[(dpte)_2Ru^{II}Cl(L)Ru^{III}Cl(bpy)_2](PF_6)_3$, L = 4,4'-bpy, bpe, bpa. The mixed-valence II, III dimers were prepared via oxidation of the corresponding II, II dimers with use of $Ce(IV)$. In a typical preparation, 0.020 g (0.013 mmol) of $[(dpte)_2ClRu^{II}(4,4'-bpy)Ru^{III}(bpy)_2](PF_6)_2$ (4,4'-bpy) $Ru^{II}(bpy)_2](PF_6)_2$ was dissolved in 3 mL of freshly distilled acetonitrile containing a 5% molar excess of once-recrystallized G. F. Smith ceric ammonium nitrate (0.0096 g, 0.020 mmol) and 2 drops of concentrated HPF_6 (Alfa-Ventron). After 5 min the solution was filtered into 20 mL of stirring anhydrous ether and the yellow-orange product $[(dpte)_2ClRu^{II}(4,4'-bpy)Ru^{III}Cl(bpy)_2](PF_6)_3$ was isolated by filtration; yield 0.0195 g, 90%. Too large an excess of Ce^{IV} led to formation of the green III, III dimer. The crude material was purified by repeated precipitations in which the product was dissolved in a dilute solution of HPF_6 in acetonitrile and filtered into 6 volumes of stirring anhydrous ether. The mixed-valence dimers undergo a spontaneous decomposition in the solid state, which gives insoluble impurities even when they are stored under vacuum. Consequently, they were either freshly prepared or freshly reprecipitated just prior to any spectroscopic or electrochemical investigations.

Luminescence Measurements. Emission spectra were all obtained on an SLM single photon counting spectrofluorimeter using a Houston Instruments X-Y recorder. All spectra were taken at room temperature in 40% dichloromethane/60% acetonitrile purged of oxygen via argon bubbling (at least 20 min of bubbling). Because of the relative weakness of the emissions observed, the instrument was run with the slits set at 16

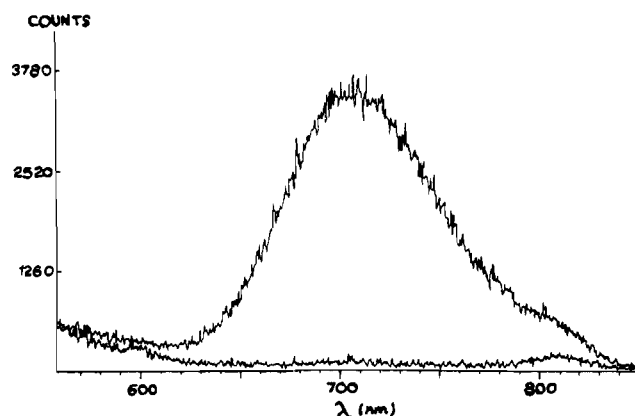


Figure 1. Emission spectrum of $[(bpy)_2ClRu^{II}(4,4'-bpy)](PF_6)$ in 60% acetonitrile/40% dichloromethane by volume at 23 ± 2 °C.

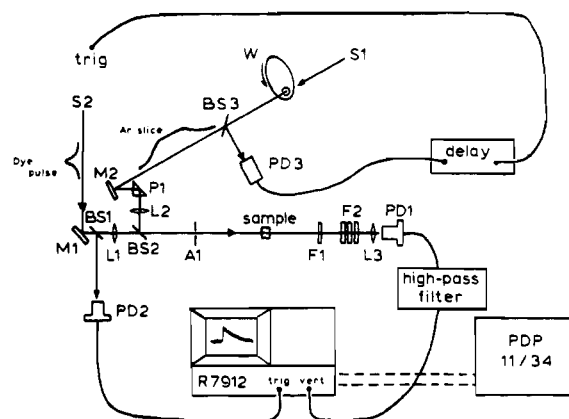


Figure 2. Schematic representation of the apparatus used in the transient absorbance experiments: S1, dye laser pulse (5 ns fwhm); S2, argon ion laser beam; W, 6.5-Hz chopping wheel; F1, dielectric filter; F2, Corning filters; P1, right-angle prism, PD3, photodiode-op amp; PD1, PD2, 50- ω high-speed photodiodes; M1, M2, dielectric mirrors; L1, 500 mm focal length lens; L2, 380 nm focal length lens; L3, 50-mm lens; BS1, BS3, uncoated silica plate; BS2, dichroic beam splitter, A1, 3-mm aperture.

mm and with the PMT voltage at the high end of the allowable range (1250 V). A typical spectrum and the background trace for the solvent mixture used are shown in Figure 1. The small feature at 810 nm present in both the spectrum and the background appears to be an instrumental artifact.

The spectra were obtained on solutions that were adjusted so that the absorbance at the 457-nm excitation wavelength was 0.1. This allowed the intensities of the observed emissions to be estimated relative to that of $[(bpy)_2Ru^{II}Cl(4,4'-bpy)]^+$ (=1.0).

Solvent Mixture. The transient absorbance and luminescence studies were all performed in a medium of 40% dichloromethane/60% acetonitrile that had been degassed via bubbling with argon (the argon was purified by passing it over a activated BTS catalyst column). The reason for the use of the mixture was to depress the freezing point of the medium so that studies could be carried out at 220 K and yet ready solubility of the complexes could be maintained. The freezing point of the mixture was found to be approximately 205 K.

The quality of the acetonitrile used in the mixture was critical since any reducing impurities led to the rapid reduction of the mixed-valence dimers $[(dpte)_2ClRu^{II}(L)Ru^{III}Cl(bpy)_2]^{3+}$. Two sources of acetonitrile were found to be satisfactory. One was commercially available Burdick and Jackson distilled in glass UV acetonitrile. The other was J. T. Baker Photrex acetonitrile that had been distilled once at high reflux ratio from fresh P_2O_5 and then once at high reflux ratio from calcium hydride. Fisher ACS certified reagent grade methylene chloride was found to be satisfactory in all cases.

Transient Absorbance Measurements. The excitation source was a pulsed dye laser tunable from 360 to 750 nm, and the monitoring light source, a continuous-wave Coherent Radiation Model CR12 argon ion laser that allows the substitution of a low-noise, high-speed photodiode for a photomultiplier tube. The wavelengths available from the argon ion laser are lines at 458, 466, 476.5, 488, 496.5, and 514.5 nm. A 400-kW nitrogen laser (Moletron UV400) was used to pump the dye laser (Moletron DL-200), which gave pulses of approximately 5 ns fwhm

(7) (a) Sullivan, B. P.; Salmon, D. J.; Meyer, T. J. *Inorg. Chem.* **1978**, *17*, 3334. (b) McCall, G. H. *Rev. Sci. Instrum.* **1973**, *43*, 865.

and between 100 and 800 mJ of energy (depending upon the output wavelength).

The objective of the various optical components in Figure 2 was to achieve collinearity of the dye laser pulse and the argon laser beams, pass the resulting double beam through the sample, and then strip away any remaining light at the excitation wavelength from the argon beam prior to detection. The dye laser output was elevated with respect to the experimental plane, and in practice mirror M1 was replaced by a two-mirror beam splitter, which both translates the pulses to the experimental plane and turns them parallel to the desired light path. Two 2-mm apertures were mounted at reproducible and identical heights on a triangular optical bench, which mounts several of the components between L1 and PD1. The apertures established an experimental axis that could be reestablished at any time. The dye laser beam was aligned with the use of adjustable mirror mounts to pass through the apertures. Lens L1 is a 500 mm focal length fused silica lens included to gently focus the dye laser pulse, and aperture A1 is a 3-mm aperture that is in place during the experiment (the alignment apertures were removed) to block off-axis reflections and the "wings" of the dye laser pulse. The argon ion laser beam was chopped by a rotating disk with a single aperture of about 5 mm width. The disk was rotated at 6.5 Hz, and the size of the aperture limited the transmitted light to about 2-ms duration. The chopped beam was brought perpendicular to the experimental axis by M2 and P1 and then reflected off the dichroic beam splitter BS2. The dichroic beam splitters used in this segment of the optical train were all dielectric, short-wavelength-pass filters, which dictated that the pump (dye laser) wavelength be shorter than the probe wavelength. To separate the residual pump radiation from the probe radiation, the long-wavelength-pass dielectric filter F1 was used, followed by appropriate Corning absorption filters F2 to attenuate the pump radiation below the limit of detectability by the photodiode PD1.

Lens L2 was a 380 mm focal length glass lens, and the positions of L1 and L2 were adjusted so that the volume sampled by the probe beam was of slightly smaller diameter and was concentric with the volume irradiated by the excitation pulse. For samples with a strong absorption at the probe wavelength, L2 was adjusted so that the focus of the probe beam did not fall within the sample to avoid thermal lensing effects. Lens L3 (50 mm focal length) was in an X-Y positioner so that the probe beam (about 2 mm in diameter at this point) was focused and positioned directly onto the active region of the photodiode contained within the coaxial photodiode mount PD1. The high-speed coaxial mounts were constructed from the design of McCall^{7b} and had sub-nanosecond rise times. Two fused silica plates (BS1, BS3) deflected a small portion (<10%) of the incident light to either a coaxial photodiode (PD2) or a Molecron Model 141 photodiode-op-amp detector (PD3), which provided the necessary timing signals described below.

The desired sequence of events has the dye laser pulse arriving at the sample during a period of constant probe intensity with the sweep on the transient digitizer (Tektronix R7912) triggered before the dye laser pulse so that the transient occurs well into the sweep. The sequence was achieved with use of PD3 to detect the rising edge of the probe beam and initiate a 1-ms digital electronic delay. The delayed output of the delay generator initiated the nitrogen laser pulse (with an internal delay of about 400 ns) which pumps the dye laser, promptly giving a laser pulse. Triggering of the transient digitizer was accomplished either with the delayed output from the delay generator or with the output of the high-speed photodiode PD2. For short events ($\tau < 40$ ns) it was advantageous to have the low-jitter trigger of the photodiode detecting the dye laser pulse rather than the 5-ns command jitter internal to the UV400.

The Tektronix transient digitizer was interfaced to a Digital Equipment Corp. PDP11/34 minicomputer and controlled with programs written in Tektronix SPS Basic. Stored wave forms were converted to absorbance units and fitted to a single exponential by a nonlinear-least-squares fitting routine.

The pulsed dye laser was operated with use of the following dyes: BBQ (386 nm), bis-MSB (417 nm), 7D4MC (457 nm). Temperature control was accomplished with an Oxford Instruments DC5159 PTC cryostat.

Results

Electrochemical Measurements. In Figure 3 are shown cyclic voltammograms for the dimer $[(dpte)_2ClRu(4,4'-bpy)RuCl(bpy)_2](PF_6)_2$ and its component monomers. As is evident in the figure and the data in Table II, the potentials of the waves in the dimer are not significantly different from those of the monomers, which is true in general for the compounds listed in Table II with only slight deviation. This is a characteristic feature for mixed-valence ions where electrostatic and resonance stabilization effects are small and thus provides evidence that electronic coupling

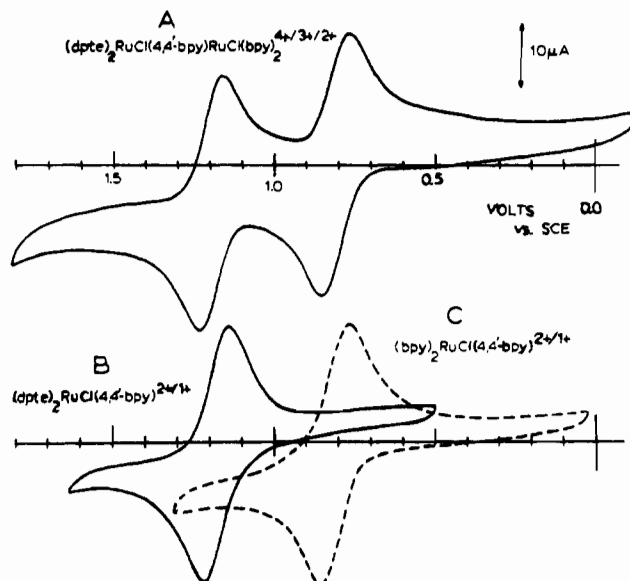


Figure 3. Cyclic voltammograms for $[(dpte)_2Ru^{II}Cl(4,4'-bpy)Ru^{II}Cl(bpy)_2](PF_6)_2$ (A), $[(dpte)_2Ru^{II}Cl(4,4'-bpy)](PF_6)$ (B), and $[(bpy)_2Ru^{II}Cl(4,4'-bpy)](PF_6)$ (C). All are at 200 mV/s in 0.1 TBAH/acetonitrile.

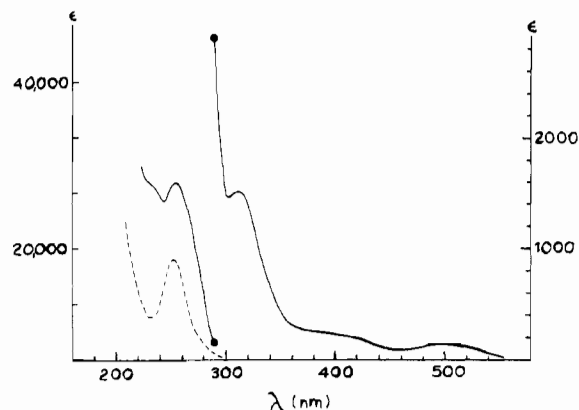


Figure 4. UV-vis spectra of the *trans*- $[(dpte)_2Ru^{II}Cl_2]$ starting material and the dpte free ligand in acetonitrile.

between the two sites is small in the ground state.

A feature that does change, however, is the average peak splitting ΔE_p between the oxidative and reductive current maxima for a given wave. For the pentaammine couples ΔE_p values increase from between 80 and 100 mV at 200 mV/s sweep rate to ΔE_p greater than 120 mV, upon incorporation into a dimer, independent of the bridging ligand. The same trend is observed, although to a lesser degree, for the $Ru(bpy)_2(Cl)L^{2+/+}$ and $Ru-(dpte)_2(Cl)L^{2+/+}$ couples, where the changes are typically from $\Delta E_p = 60$ –80 mV for the monomers to $\Delta E_p = 100$ for the dimers. The origin of the apparent enhanced inhibition to electron transfer in the dimers is not known. Agreement between values reported here and those reported earlier for some of the compounds are in satisfactory agreement.^{4a,8}

UV-Vis Spectra. The spectra of the $[(NH_3)_5Ru^{II/III}(L)-Ru^{II}Cl(bpy)_2]^{3+/4+}$ dimers and the $[(bpy)_2Ru^{II}Cl(L)]^+$ monomers have been discussed previously.^{4,9} However, certain features of the spectra are important here, and spectral data (λ_{max} , ϵ_{max}) for all of the compounds studied are listed in supplementary table 3. Figures 4–6 show representative examples of spectra for the complexes.

The spectrum of the *trans*- $[(dpte)_2Ru^{II}Cl_2]$ starting material is dominated by a strong ($\epsilon_{max} = 3.2 \times 10^4 M^{-1} cm^{-1}$) absorption

(8) Powers, M. J. Ph.D. Dissertation, The University of North Carolina, Chapel Hill, NC, 1977.

(9) Johnson, E. C. Ph.D. Dissertation, The University of North Carolina, Chapel Hill, NC, 1975.

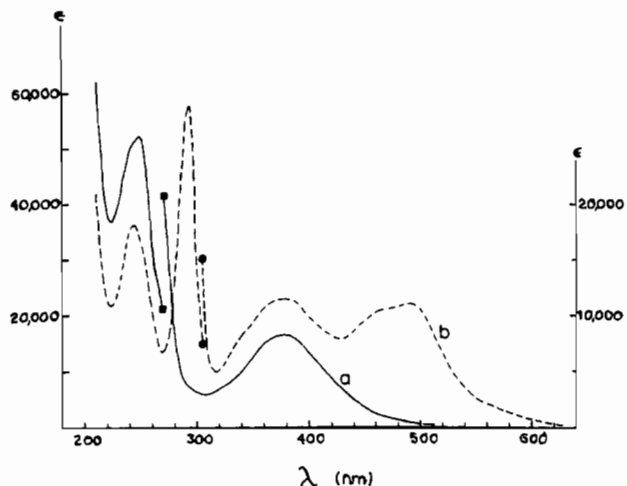


Figure 5. UV-vis spectra of the monomeric complexes $[(dpte)_2Ru^{II}Cl(4,4'-bpy)]PF_6$ (a) and $[(bpy)_2Ru^{II}Cl(4,4'-bpy)]PF_6$ (b) in acetonitrile.

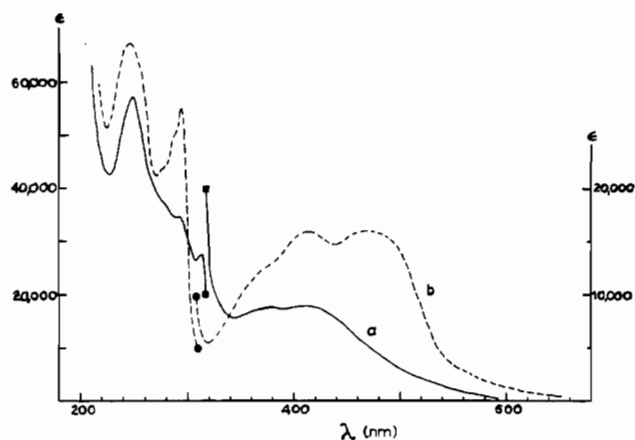


Figure 6. UV-vis spectra of the dimeric complexes $[(dpte)_2ClRu^{II}(4,4'-bpy)Ru^{III}Cl(bpy)_2](PF_6)_3$ (a) and $[(dpte)_2ClRu^{II}(4,4'-bpy)Ru^{II}Cl(bpy)_2](PF_6)_2$ in acetonitrile.

band centered at 256 nm which is also present in the free ligand and can be assigned to a ligand-localized $\pi-\pi^*$ transition based on the phenyl groups. The band at 313 nm with $\epsilon = 1.51 \times 10^3 \text{ M}^{-1} \text{ cm}^{-1}$ is probably $S \leftarrow d(Ru^{II})$ MLCT (metal-to-ligand charge transfer) in character with the acceptor orbital on sulfur being either $3d$ or σ^* . Taube and co-workers have shown the existence of such MLCT transitions in complexes like $[(NH_3)_5Ru^{II}S(CH_3)_2]^{2+}$.¹⁰ The assignment is consistent with the fact that the band disappears in the spectrum of the nitrile complex $[(dpte)_2Ru^{II}Cl(NCCH_3)]^+$, since the higher redox potential at the metal (1.33 vs. 0.62 V) is expected to raise the energy of the transition into the intense $\pi-\pi^*$ absorption region of the sulfur ligand. The other two weak bands at 415 and 498 nm have been assigned as $d-d$ transitions ${}^1E \leftarrow {}^1A_1$ and ${}^1A_2 \leftarrow {}^1A_1$ by Chatt et al.⁶

In the complexes $[(dpte)_2Ru^{II}Cl(L)]^+$, where $L = 4,4'$ -bpy, bpe, bpa, the UV spectra are a composite of the $\pi-\pi^*$ band of the sulfur chelate and the $\pi-\pi^*$ bands of the nitrogen heterocycles. In the near-UV region each has the strong, broad peak expected for a $\pi^*(L) \leftarrow d\pi(Ru^{II})$ MLCT transition. In all cases it is significantly more intense and is at lower energy than the $S \leftarrow d\pi$ transition seen in the dichloride. The $S \leftarrow d\pi$ transition is not observed, presumably because it is masked by the $\pi^*(L) \leftarrow d\pi(Ru^{II})$ band or shifted into the $\pi-\pi^*$ region due to the increased $Ru(III/II)$ redox potential at the metal site, which is a consequence of the substitution of a back-bonding pyridyl ligand for Cl^- . The MLCT bands are sufficiently intense that the $d-d$ bands are masked. The spectra of the dimers are a complicated composite of the absorption

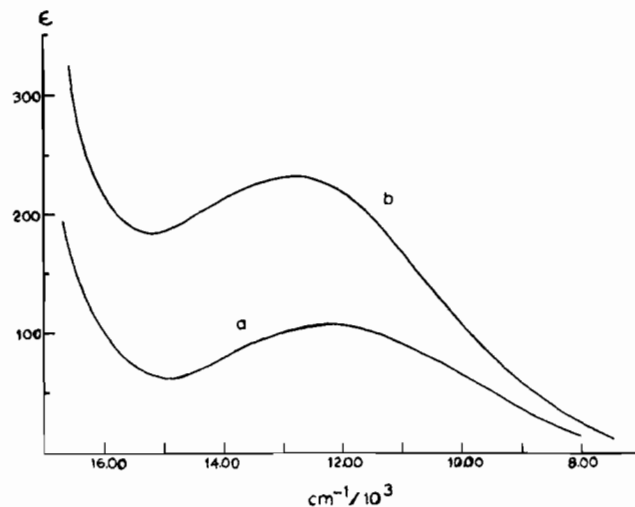


Figure 7. Near-infrared spectra for the mixed-valence dimers $[(dpte)_2Ru^{II}Cl(4,4'-bpy)Ru^{III}Cl(bpy)_2](PF_6)$ (a) and $[(dpte)_2Ru^{II}Cl(bpe)Ru^{III}Cl(bpy)_2](PF_6)_3$ (b).

bands of the component monomers. In the $Ru(II)-Ru(II)$ dimers the visible spectrum is dominated by $\pi^*(bpy) \leftarrow d\pi(Ru^{II})$ transitions at the $[(bpy)_2ClRu^{II}(L)]^+$ site but there are subtle changes in band shapes and energies for the transitions in the dimers.^{4,8,9} As for the monomers, the ultraviolet region is a mixture of overlapping bands arising from $\pi^* \leftarrow \pi(dpte)$, $\pi^* \leftarrow \pi(L)$, and $\pi^* \leftarrow \pi(bpy)$ transitions.

In the II, III dimers visible spectra are somewhat simplified because of the disappearance of the intense $\pi^*(bpy) \leftarrow d\pi(Ru(II))$ transitions. Note Figure 6. The electrochemical results in Table II show that in the mixed-valence dimers the odd electron in the system is localized on the $(dpte)_2ClRu^{II}$ end of the dimer due to the large redox asymmetry of ~ 0.4 V, imposed by the differences in ligands at the two sites. In the mixed-valence dimers a relatively weak band is observed at about 420 nm with a band at slightly higher energy associated with the $\pi^*(L) \leftarrow d\pi((dpte)_2Ru^{II}Cl^+)$ transition at the $Ru(II)$ sites.

The peak at 420 nm is a $d\pi(Ru) \leftarrow p\pi(Cl^-)$ LMCT (ligand-to-metal charge transfer) transition arising at the $-Ru^{III}Cl(bpy)_2$ end of the dimer with perhaps a contribution from $d\pi(Ru^{III}) \leftarrow \pi(\text{ligand})$ transitions involving the pyridyl ligands.

As for related monomers, in the UV, the intense $\pi^* \leftarrow \pi(bpy)$ transition for the II, II dimer at 293 nm splits into two somewhat less intense peaks at slightly lower energies upon oxidation of the Ru -bpy site to Ru^{III} .

Near-Infrared (Near-IR) Spectra. In Figure 7 are shown intervalence-transfer (IT) bands for the dimers $[(dpte)_2Cl(L)Ru^{III}Cl(bpy)_2]^{3+}$, where $L = 4,4'$ -bpy and bpe, which occur at 823 nm ($\epsilon = 110 \text{ M}^{-1} \text{ cm}^{-1}$) and 781 nm ($\epsilon = 232 \text{ M}^{-1} \text{ cm}^{-1}$), respectively. The shift to higher energy for the bpe-bridged dimer is expected, given the longer separation between metals.¹¹ For the unsymmetrical dimers $[(NH_3)_5Ru^{III}(L)Ru^{II}Cl(bpy)_2]^{4+}$ the IT band overlaps strongly with the tail of the $\pi^*(bpy) \leftarrow d\pi(Ru^{II}Cl(bpy)_2)$ MLCT band, making it difficult to resolve a well-defined absorption maximum.

For the $4,4'$ -bpy- and bpe-bridged dimers, $[(dpte)_2ClRu^{II}(L)Ru^{III}Cl(bpy)_2]^{3+}$, the best estimate for the extinction coefficients for the IT bands corrected for residual absorbance due to the low-energy tail of the $\pi^*(bpy) \leftarrow d\pi(Ru^{II}Cl(bpy)_2)$ MLCT band is $90 \pm 5 \text{ M}^{-1} \text{ cm}^{-1}$ ($4,4'$ -bpy) and $210 \pm 10 \text{ M}^{-1} \text{ cm}^{-1}$ (bpe). The band widths at half-maximum, obtained by doubling the low-energy side, are 5.06×10^3 ($4,4'$ -bpy) and 4.9×10^3 (bpe), which are within 10% of the values calculated from the classical equation given by Hush¹²

$$\Delta\nu_{1/2}(\text{theor}) = 2.31 \times 10^3(E_{op} - \Delta E) \quad (1)$$

(10) (a) Kuehn, C. G.; Taube, H. *J. Am. Chem. Soc.* **1976**, *98*, 689. (b) Stein, C. A.; Taube, H. *Inorg. Chem.* **1979**, *18*, 2212.

(11) Sullivan, B. P.; Curtis, J. C.; Kober, E. M.; Meyer, T. J. *Nouv. J. Chim.* **1980**, *4*, 643-650.

(12) Hush, N. S. *Prog. Inorg. Chem.* **1961**, *8*, 391.

Table III. Luminescence Data at $23 \pm 2^\circ\text{C}$ in 40% Methylene Chloride/60% Acetonitrile (Argon Deoxygenated)^a

ion	emission λ_{max} , nm	approx rel intens ^b
$[(\text{bpy})_2\text{Ru}^{\text{II}}\text{Cl}(4,4'\text{-bpy})]^+$	698 ± 5	1.0
$[(\text{NH}_3)_5\text{Ru}^{\text{II}}(4,4'\text{-bpy})\text{Ru}^{\text{II}}\text{Cl}(\text{bpy})_2]^{3+}$	~ 700	c
$[(\text{NH}_3)_5\text{Ru}^{\text{III}}(4,4'\text{-bpy})\text{Ru}^{\text{II}}\text{Cl}(\text{bpy})_2]^{4+}$	~ 700	c
$[(\text{dpte})_2\text{Ru}^{\text{II}}\text{Cl}(4,4'\text{-bpy})\text{Ru}^{\text{II}}\text{Cl}(\text{bpy})_2]^{2+}$	706 ± 10	0.2
$[(\text{dpte})_2\text{Ru}^{\text{II}}\text{Cl}(4,4'\text{-bpy})\text{Ru}^{\text{III}}\text{Cl}(\text{bpy})_2]^{3+}$	708 ± 10	0.2
$[(\text{bpy})_2\text{Ru}^{\text{II}}\text{Cl}(\text{bpe})]^+$	697 ± 5	0.2
$[(\text{NH}_3)_5\text{Ru}^{\text{II}}(\text{bpe})\text{Ru}^{\text{II}}\text{Cl}(\text{bpy})_2]^{3+}$	~ 700	c
$[(\text{NH}_3)_5\text{Ru}^{\text{III}}(\text{bpe})\text{Ru}^{\text{II}}\text{Cl}(\text{bpy})_2]^{4+}$	~ 700	c
$[(\text{dpte})_2\text{Ru}^{\text{II}}\text{Cl}(\text{bpe})\text{Ru}^{\text{II}}\text{Cl}(\text{bpy})_2]^{2+}$	700 ± 5	0.1
$[(\text{dpte})_2\text{Ru}^{\text{II}}\text{Cl}(\text{bpe})\text{Ru}^{\text{III}}\text{Cl}(\text{bpy})_2]^{3+}$	704 ± 10	0.1
$[(\text{bpy})_2\text{Ru}^{\text{II}}\text{Cl}(\text{bpa})]^+$	707 ± 10	0.6
$[(\text{NH}_3)_5\text{Ru}^{\text{II}}(\text{bpa})\text{Ru}^{\text{II}}\text{Cl}(\text{bpy})_2]^{3+}$	711 ± 10	0.2
$[(\text{NH}_3)_5\text{Ru}^{\text{III}}(\text{bpa})\text{Ru}^{\text{II}}\text{Cl}(\text{bpy})_2]^{4+}$	713 ± 10	0.5
$[(\text{dpte})_2\text{Ru}^{\text{II}}\text{Cl}(\text{bpa})\text{Ru}^{\text{II}}\text{Cl}(\text{bpy})_2]^{2+}$	706 ± 10	0.5
$[(\text{dpte})_2\text{Ru}^{\text{II}}\text{Cl}(\text{bpa})\text{Ru}^{\text{III}}\text{Cl}(\text{bpy})_2]^{3+}$	704 ± 10	0.5
$[(\text{NH}_3)_5\text{Ru}^{\text{II}}(4,4'\text{-bpy})]^{2+}$		d
$[(\text{dpte})_2\text{Ru}^{\text{II}}\text{Cl}(4,4'\text{-bpy})]^+$		d

^a The solution concentrations were adjusted so that the absorbance was 0.1 at the excitation wavelength of 457 nm. ^b Relative to $[(\text{bpy})_2\text{Ru}^{\text{II}}\text{Cl}(4,4'\text{-bpy})]^+$ as the standard with $\phi_{\text{em}} < 1 \times 10^{-3}$. ^c Very weak emission (relative intensity < 0.1); probably due to trace amounts of the monomeric complex $[(\text{bpy})_2(\text{L})\text{Ru}^{\text{II}}\text{Cl}]^+$. ^d No detectable emission.

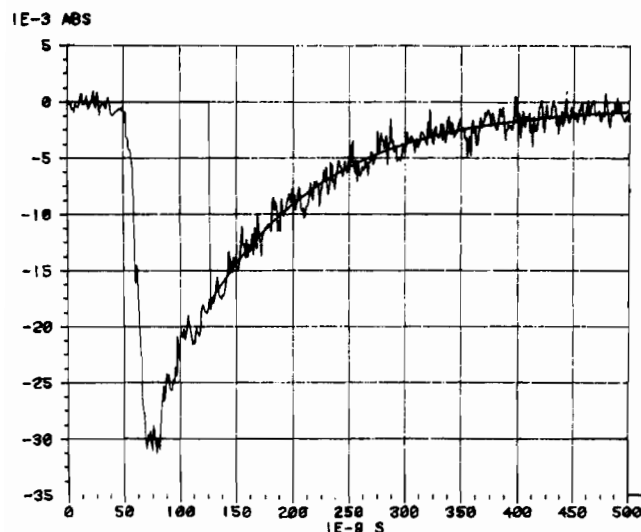


Figure 8. Transient absorbance decrease at 514 nm following 547-nm photolysis (5-ns pulse) of the $[(\text{bpy})_2\text{Ru}^{\text{II}}\text{Cl}(4,4'\text{-bpy})]\text{PF}_6$ monomer at 250 K in argon-degassed 60% acetonitrile/40% methylene chloride. $\tau = 103 \pm 15$ ns.

In the calculations, the difference in potentials for the redox couples for the two ends of the dimer was used as an estimate of ΔE . E_{op} is the energy at maximum absorbance.

The extent of electronic delocalization between the Ru(II) and Ru(III) sites, α^2 , can be estimated from¹²

$$\alpha^2 = \frac{4.24 \times 10^{-20} \epsilon_{\text{max}} \Delta\nu_{1/2}}{E_{\text{op}}(d^2)} \quad (2)$$

where d is the distance between the sites in cm. The distance in the 4,4'-bpy system is estimated at 11.1×10^{-8} cm,³ thus giving $\alpha^2 = 1.2 \times 10^{-4}$ (4,4'-bpy) and $\alpha^2 = 2.0 \times 10^{-4}$ (bpe). The values are typical of those obtained in related mixed-valence systems.¹³⁻¹⁶

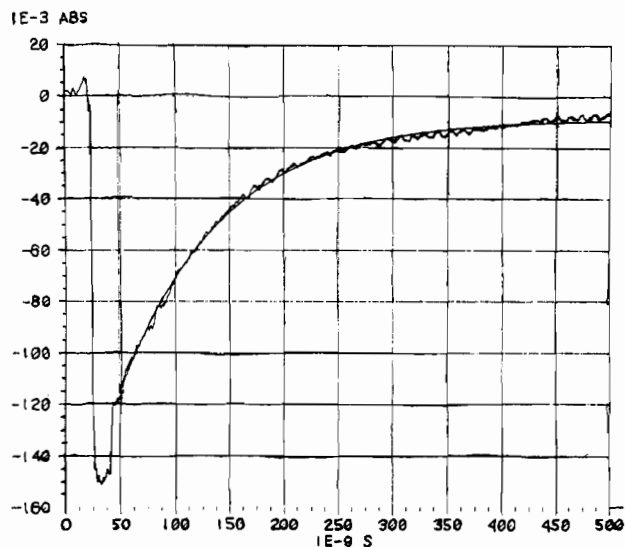


Figure 9. Transient absorbance decrease at 514 nm obtained following 457-nm photolysis (5-ns pulse) of the dimer $[(\text{dpte})_2\text{ClRu}^{\text{II}}(4,4'\text{-bpy})\text{-Ru}^{\text{II}}(4,4'\text{-bpy})]\text{PF}_6$ at 250 K in argon-degassed 60% acetonitrile/40% methylene chloride. $\tau = 96 \pm 15$ ns.

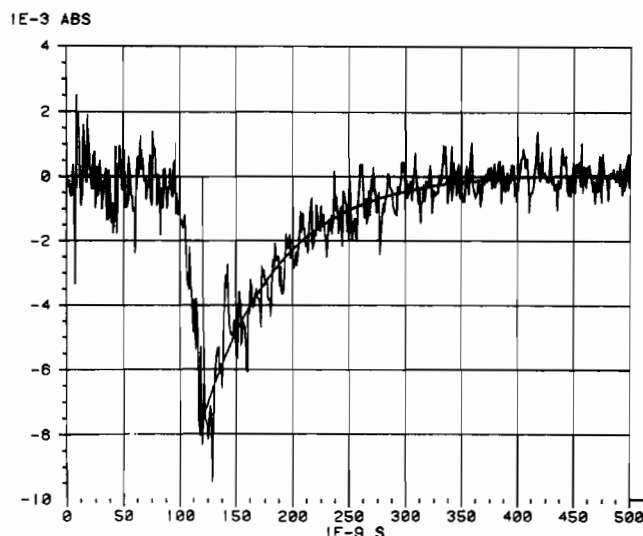


Figure 10. Transient absorbance decrease at 476 nm obtained following 417-nm photolysis (5-ns pulse) of the mixed-valence dimer $[(\text{dpte})_2\text{ClRu}^{\text{II}}(4,4'\text{-bpy})\text{Ru}^{\text{III}}(4,4'\text{-bpy})]\text{PF}_6$ at 250 K in argon-degassed 60% acetonitrile/40% methylene chloride. $\tau = 104 \pm 25$ ns.

Luminescence Measurements. Luminescence data obtained for the compounds are summarized in Table III, and a typical spectrum is shown in Figure 1. The emission intensities are relatively weak in all cases. Comparing the observed emission intensity (at 700 nm) from $[(\text{bpy})_2\text{Ru}^{\text{II}}\text{Cl}(4,4'\text{-bpy})]^+$ with that obtained from an equally optically dense sample of $[\text{Ru}^{\text{II}}(\text{bpy})_3]^{2+}$ at the excitation wavelengths of 457 nm allows an upper limit of $\phi_{\text{em}} < 1 \times 10^{-3}$ to be placed on the luminescence efficiency for the chloro complex.¹⁷

Transient Absorbance Data. Transient absorbance changes produced by irradiation of the various monomers and dimers were observed with use of the apparatus and technique described in the Experimental Section. The data are summarized in Table IV. In nearly all cases where transients were observed, photolysis produces a transient bleaching in the MLCT region where the starting Ru(II) monomers and dimers absorb strongly. From the data in Figure 8-10 it is apparent that the absorbance of the solution at the monitoring wavelength decreases within the duration of the dye laser pulse (~ 5 ns) and then slowly (relative

(13) Powers, M. J.; Meyer, T. J. *J. Am. Chem. Soc.* **1980**, *102*, 1289.

(14) Sullivan, B. P.; Meyer, T. J. *Inorg. Chem.* **1980**, *19*, 752.

(15) Curtis, J. C.; Meyer, T. J. *J. Am. Chem. Soc.* **1978**, *100*, 6284.

(16) Callahan, R. W.; Keene, F. R.; Meyer, T. J.; Salmon, D. J. *J. Am. Chem. Soc.* **1977**, *99*, 1064.

(17) Durham, W. B.; Caspar, J. V.; Nagle, J. K.; Meyer, T. J. *J. Am. Chem. Soc.* **1982**, *104*, 4803.

Table IV. Lifetime Data (in ns) for Transient Absorption Changes following Laser Flash Photolysis in 40% Methylene Chloride/60% Acetonitrile (Argon Deoxygenated)

ion ^a	τ (220 K), ns	τ (250 K), ns	τ (280 K), ns
$[(\text{bpy})_2\text{Ru}^{\text{II}}\text{Cl}(4,4'\text{-bpy})]^+$	143 ± 20^b	103 ± 15	74 ± 20
$[(\text{NH}_3)_5\text{Ru}^{\text{II}}(4,4'\text{-bpy})\text{Ru}^{\text{II}}\text{Cl}(\text{bpy})_2]^{3+}$	<i>c</i>		
$[(\text{NH}_3)_5\text{Ru}^{\text{III}}(4,4'\text{-bpy})\text{Ru}^{\text{II}}\text{Cl}(\text{bpy})_2]^{4+}$	100 ± 20	<i>d</i>	<i>d</i>
$[(\text{dpte})_2\text{ClRu}^{\text{II}}(4,4'\text{-bpy})\text{Ru}^{\text{II}}\text{Cl}(\text{bpy})_2]^{2+}$	140 ± 15	96 ± 15	51 ± 10
$[(\text{dpte})_2\text{ClRu}^{\text{II}}(4,4'\text{-bpy})\text{Ru}^{\text{III}}\text{Cl}(\text{bpy})_2]^{3+}$	155 ± 30	104 ± 25	54 ± 20
$[(\text{bpy})_2\text{Ru}^{\text{II}}\text{Cl}(\text{bpe})]^+$	147 ± 10	120 ± 10	102 ± 10
$[(\text{NH}_3)_5\text{Ru}^{\text{II}}(\text{bpe})\text{Ru}^{\text{II}}\text{Cl}(\text{bpy})_2]^{3+}$	<i>c</i>		
$[(\text{NH}_3)_5\text{Ru}^{\text{III}}(\text{bpe})\text{Ru}^{\text{II}}\text{Cl}(\text{bpy})_2]^{4+}$	116 ± 15	<i>d</i>	59 ± 15
$[(\text{dpte})_2\text{Ru}^{\text{II}}\text{Cl}(\text{bpe})\text{Ru}^{\text{II}}\text{Cl}(\text{bpy})_2]^{2+}$	59 ± 20	57 ± 20	60 ± 20
$[(\text{dpte})_2\text{ClRu}^{\text{II}}(\text{bpe})\text{Ru}^{\text{III}}\text{Cl}(\text{bpy})_2]^{3+e}$	83 ± 30	70 ± 30	50 ± 20
$[(\text{bpy})_2\text{Ru}^{\text{II}}\text{Cl}(\text{bpa})]^+$	100 ± 20	92 ± 20	85 ± 15
$[(\text{NH}_3)_5\text{Ru}^{\text{II}}(\text{bpa})\text{Ru}^{\text{II}}\text{Cl}(\text{bpy})_2]^{3+}$	122 ± 25	98 ± 25	74 ± 20
$[(\text{NH}_3)_5\text{Ru}^{\text{III}}(\text{bpa})\text{Ru}^{\text{II}}\text{Cl}(\text{bpy})_2]^{4+}$	113 ± 35	<i>d</i>	<i>d</i>
$[(\text{dpte})_2\text{ClRu}^{\text{II}}(\text{bpa})\text{Ru}^{\text{II}}\text{Cl}(\text{bpy})_2]^{2+}$	102 ± 15	97 ± 15	64 ± 15
$[(\text{dpte})_2\text{ClRu}^{\text{II}}(\text{bpa})\text{Ru}^{\text{III}}\text{Cl}(\text{bpy})_2]^{3+}$	110 ± 30	<i>d</i>	<i>d</i>

^a In all cases the counterion was PF_6^- . ^b Error limits reflect a combination of the standard deviations of multiple runs at each temperature and the variability of the lifetimes obtained from a single trace as a function of the limits of analysis over which the computer fit was performed. ^c No observable transient. ^d For these transients, the signals were sufficiently weak that no quantitative analysis of the decay time was possible. ^e Signal may be due in part to the 2,2 reduction product.

to the length of the exciting pulse) returns to the initial value with a characteristic exponential decay. The dimers are photochromic under these conditions, and no further transient absorbance changes are observed at longer time scales to within an estimated experimental sensitivity of $\pm 10\%$. The transient behavior observed must represent a repopulation of the ground state from thermally equilibrated states reached following excitation by the laser pulse. For complexes that absorb strongly in the region near 490 nm—the $[(\text{bpy})_2\text{Ru}^{\text{II}}\text{Cl}(\text{L})]^+$ monomers and the $[(\text{NH}_3)_5\text{Ru}^{\text{III/II}}(\text{L})\text{Ru}^{\text{II}}\text{Cl}(\text{bpy})_2]^{2+}$ dimers—the excitation pulse used was 457 nm, and the probe was the 514-nm line from the argon ion laser. For those complexes that had their maximum absorbance in the near UV—the $[(\text{dpte})_2\text{ClRu}^{\text{II}}(\text{L})\text{Ru}^{\text{III}}\text{Cl}(\text{bpy})_2]^{3+}$ dimers—the pulse was at 417 nm and the probe used was either the 476- or the 514-nm argon ion laser line.

The intensity change for a given molecule was dependent upon the wavelengths used as expected given the wavelength dependencies of the extinction coefficients and of the excitation pulses of the exciting and interrogating beams. However, the transient lifetimes were independent of the wavelengths of both beams, showing that although the extent of population of the transiently observed excited state may be wavelength dependent, the excited state ultimately reached and the transient decay process observed are independent of irradiating wavelength. This applies rigorously only over a range from 380 to 460 nm since no excitations were performed outside these limits.

Laser flash photolysis of the monomers $[(\text{dpte})_2\text{Ru}^{\text{II}}\text{Cl}(\text{L})]^+$, in the region of their MLCT bands, gave no evidence for any transient absorbance change even during the lifetime of the excitation pulse (~ 5 ns), nor did their excitation give rise to observable luminescence. It seems reasonable to conclude that the $\pi^*(\text{L}) \leftarrow d\pi(\text{Ru}^{\text{II}})$ MLCT excited states reached upon irradiation are probably very short lived.

The monomeric complexes $[(\text{bpy})_2\text{Ru}^{\text{II}}\text{Cl}(\text{L})]^+$ show strong transient bleaching upon photolysis (457-nm excitation, 514-nm probe) and also exhibit an easily detectable luminescence in fluid solution at room temperature. A typical decay curve is shown for the 4,4'-bpy monomer in Figure 8.

When a $[(\text{NH}_3)_5\text{Ru}^{\text{III}}]^{2+}$ group is added to the bridging ligand L, the transient behavior is totally quenched in the complexes $[(\text{NH}_3)_5\text{Ru}^{\text{III}}(4,4'\text{-bpy})\text{Ru}^{\text{II}}\text{Cl}(\text{bpy})_2]^{3+}$ and $[(\text{NH}_3)_5\text{Ru}^{\text{III}}(\text{bpe})\text{Ru}^{\text{II}}\text{Cl}(\text{bpy})_2]^{3+}$. By contrast, in the bpa-bridged $\text{Ru}^{\text{II}}\text{-Ru}^{\text{II}}$ dimer a relatively intense transient was observed with a luminescence intensity about one-third that for the $[(\text{bpy})_2\text{Ru}^{\text{II}}\text{Cl}(\text{bpa})]^+$ monomer. Oxidation to the mixed-valence dimers $[(\text{NH}_3)_5\text{Ru}^{\text{III}}(\text{L})\text{Ru}^{\text{II}}\text{Cl}(\text{bpy})_2]^{4+}$ led to some interesting changes in the observed transient behavior. A very weak but definite transient absorbance decrease became observable for both the 4,4'-bpy- and bpe-bridged dimers, although the luminescence from the dimers was weak and its origin could be in trace amounts of monomeric impurities. In

the case of the bpa-bridged dimer a transient absorbance decrease was observed but the total intensity change was small and it was not possible to obtain reliable kinetic information above 220 K.

The luminescence from this mixed-valence dimer was not significantly quenched compared to that of the monomer, and it appeared to emit more strongly than the $\text{Ru}(\text{II})\text{-Ru}(\text{II})$ dimer.

The monomeric pentaammine complex $[(\text{NH}_3)_5\text{Ru}^{\text{II}}(4,4'\text{-bpy})]^{2+}$ gave an observable transient absorbance increase at 514 nm during the lifetime of the exciting pulse (~ 5 ns, 547 nm). This is in contrast to the 0.8-ns bleaching observed in the region from 560 to 600 nm upon MLCT excitation of the complex $[(\text{NH}_3)_5\text{Ru}^{\text{II}}(\text{pz})]^{2+}$ (pz = pyrazine).¹⁸ The difference may simply reflect a dissimilarity between the visible spectra of the reduced 4,4'-bpy and pz ligands. The lifetime of the excited-state absorbance could be estimated as ~ 1 ns within a rather large uncertainty, although an upper limit of 2 ns can be confidently assigned. The complex did not give rise to a detectable emission.

The $\text{Ru}(\text{II})\text{-Ru}(\text{II})$ dimers $[(\text{dpte})_2\text{ClRu}^{\text{II}}(\text{L})\text{Ru}^{\text{II}}\text{Cl}(\text{bpy})_2]^{2+}$, containing the sulfur chelate dpte, all displayed readily observable transient absorption changes following laser flash photolysis (457-nm excitation, 514-nm probe). For the 4,4'-bpy-bridged complex $[(\text{dpte})_2\text{ClRu}^{\text{II}}(4,4'\text{-bpy})\text{Ru}^{\text{II}}\text{Cl}(\text{bpy})_2]^{2+}$ the observed transient has approximately the same lifetime as the monomeric complex $[(\text{bpy})_2\text{Ru}^{\text{II}}\text{Cl}(4,4'\text{-bpy})]^+$ at 220 K. The dimer emits at approximately the same energy as the monomer (~ 700 nm), but the intensity of the luminescence is decreased by a factor of about 5.

With bpe as the ligand bridge, inspection of Table IV shows that the lifetime for the $\text{Ru}(\text{II})\text{-Ru}(\text{II})$ dimer ($\tau(220 \text{ K}) = 59 \pm 20$ ns) is significantly lowered compared to that for the monomer (147 ± 10 ns) and becomes temperature independent. Luminescence is still observed in the dimer at approximately the same wavelength (~ 700 nm) and intensity (within a factor of 2) as for the monomer $[(\text{bpy})_2\text{Ru}^{\text{II}}\text{Cl}(\text{bpe})]^+$.

In the bpa-bridged dimer the luminescence and the transient decay properties are essentially identical with those observed for the monomer $[(\text{bpy})_2\text{Ru}^{\text{II}}\text{Cl}(\text{bpa})]^+$.

The photophysical properties of the mixed-valence dimers $[(\text{dpte})_2\text{ClRu}^{\text{II}}(\text{L})\text{Ru}^{\text{III}}\text{Cl}(\text{bpy})_2]^{3+}$ are most interesting. A point that must be made clearly is that, because of the oxidation-state distribution in the dimer, the $\pi^*(\text{bpy}) \leftarrow d\pi(\text{Ru}^{\text{II}})$ chromophore no longer exists in the mixed-valence dimers. Direct excitation into the $\pi^*(\text{bpy}) \leftarrow d\pi(\text{Ru}^{\text{II}})$ MLCT band is no longer possible, and instead, the excitation wavelength used was in the higher energy spectral region, typically at 417 nm although 380-nm excitation pulses were also employed. Photolysis of the dimer $[(\text{dpte})_2\text{ClRu}^{\text{II}}(4,4'\text{-bpy})\text{Ru}^{\text{III}}\text{Cl}(\text{bpy})_2]^{3+}$ at 417 nm gave rise to

(18) Creutz, C.; Krogen, P.; Matsubara, T.; Netzel, T. L.; Sutin, N. *J. Am. Chem. Soc.* **1979**, *101*, 5442.

Table V. Rate Constants for Quenching of the (bpy⁻)₂Ru^{III} MLCT Excited States of [(bpy)₂Ru^{II}Cl(4,4'-bpy)]⁺, [(dpte)₂ClRu^{II}(4,4'-bpy)Ru^{II}Cl(bpy)₂]²⁺, and [(dpte)₂ClRu^{II}(4,4'-bpy)Ru^{III}Cl(bpy)₂]³⁺ by *p*-CH₃⁺NC₅H₄CONH₂^a

complex	$\lambda_{\text{excitation}}$, nm	λ_{monitor} , nm	τ_0 , ns	$10^{-6}k_q$, M ⁻¹ s ⁻¹ ^b
[(bpy) ₂ ClRu ^{II} (4,4'-bpy)] ⁺	457	514	103	3.6
[(dpte) ₂ ClRu ^{II} (4,4'-bpy)Ru ^{II} Cl(bpy) ₂] ²⁺	457	514	101	2.7
[(dpte) ₂ ClRu ^{II} (4,4'-bpy)Ru ^{III} Cl(bpy) ₂] ³⁺	417	476	104	2.4

^a Measurements performed at 250 K in 40% dichloromethane/60% acetonitrile. ^b k_q calculated from the slopes of plots of $1/\tau$ vs. [Q] according to the equation $1/\tau = 1/\tau_0 + k_q[Q]$.

a transient bleaching and subsequent return to the original absorbance with a lifetime and ($\tau_0(220\text{ K}) = 155 \pm 30\text{ ns}$) within experimental error of τ_0 for the II,II dimer ($140 \pm 15\text{ ns}$). The total intensity of the absorbance change was significantly less in the mixed-valence dimer, but in large part, this is readily attributable to the smaller molar absorptivity of the complex at the 476- and 574-nm argon-ion interrogating wavelengths used.

Care was taken to ascertain that the observed transient behavior was not due simply to a small amount of the Ru(II)-Ru(II) dimer present as an impurity. The absence of the II,II dimer could be verified both before and after the experiment by noting the visible spectrum of the solution using the absence of the characteristic $\pi^*(\text{bpy}) \leftarrow d\pi(\text{Ru}^{\text{II}})$ absorption band (λ_{max} at 491 nm) as the criterion. Furthermore, solutions of the II,III ion containing Ce(IV) ion as ceric ammonium nitrate gave the same lifetime and luminescence behavior. Given the redox potentials involved, with excess Ce(IV) the solution could only contain the [(dpte)₂ClRu^{II}(4,4'-bpy)Ru^{III}Cl(bpy)₂]³⁺ and [(dpte)₂ClRu^{III}(4,4'-bpy)Ru^{III}Cl(bpy)₂]⁴⁺ dimers in any significant amount. For the mixed-valence bpe-bridged dimer, data acquisition was complicated by a marked propensity of the dimer to undergo photochemical reduction to the Ru(II)-Ru(II) form. The transient decay data differ from the values obtained for the Ru(II)-Ru(II) dimer in that there is a decrease in τ_0 ($\tau_0(220\text{ K}) = 80 \pm 30$ vs. $59 \pm 20\text{ ns}$), although the luminescence properties of the two dimers are similar.

The bpa-bridged, mixed-valence dimer gave a low-intensity, transient decay and a rather weak luminescence. The observed values for the lifetime ($110 \pm 30\text{ ns}$ at 220 K) and emission maximum ($704 \pm 10\text{ nm}$) are consistent with the results obtained for the [(bpy)₂Ru^{II}Cl(bpa)]⁺ monomer and fully reduced [(dpte)₂ClRu^{II}(bpa)Ru^{II}Cl(bpy)₂]²⁺ dimer.

Excited-State Quenching. This similarities between the transient decay and luminescence behavior observed for the Ru^{II}-Ru^{II} and mixed-valence dimers [(dpte)₂ClRu^{II}(4,4'-bpy)Ru^{II/III}Cl(bpy)₂]^{2+/3+} and the monomer [(bpy)₂Ru^{II}Cl(4,4'-bpy)]⁺ strongly suggest that the observed photophysical behavior is due to common, or at least closely related, excited states that are populated following laser flash photolysis. To further test this hypothesis, a series of Stern-Volmer quenching experiments were carried out in which the nature of the excited states observed by transient absorbance was probed chemically. The approach taken was to compare quenching rate constants with the use of a common quencher for the monomer and two dimers.

The quencher used was the oxidative electron-transfer quencher 4-amido-*N*-methylpyridinium cation (hereafter abbreviated P⁺). The pyridinium ion undergoes a reversible one-electron reduction at $E_{1/2} = -0.94\text{ V}$ vs. SCE in acetonitrile and quenches the luminescent excited state of [Ru^{II}(bpy)₃](PF₆)₂ in deaerated acetonitrile with a quenching rate constant of $4.12 \times 10^7\text{ M}^{-1}\text{ s}^{-1}$.¹⁹ The k_q value is well below the observed diffusion-limited rate constant for electron-transfer quenching in acetonitrile of $(1-2) \times 10^{10}\text{ M}^{-1}\text{ s}^{-1}$. When electron-transfer quenching rate constants are less than the diffusion-controlled limit, their magnitudes are sensitive to the free energy change of the quenching step and thus to the redox potentials of the quencher and the excited-state couples.²⁰⁻²² The reduction potential for the couple Ru-

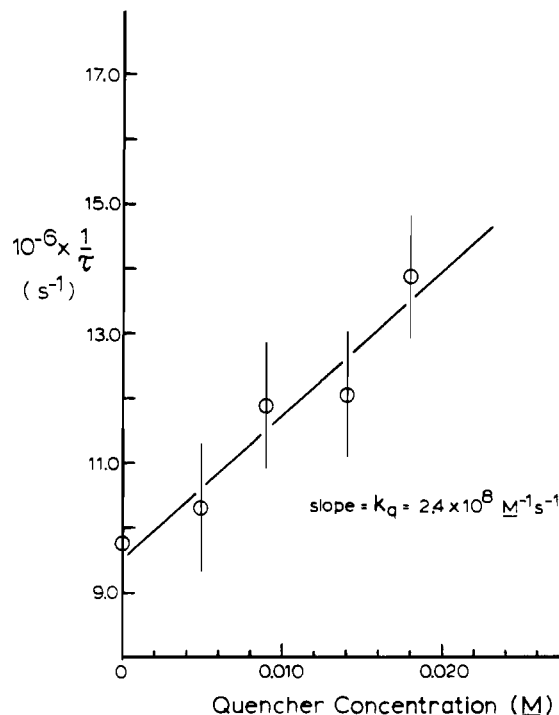
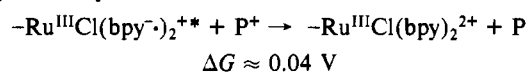


Figure 11. Plot of $1/\tau$ vs. quencher concentration for the transient excited state for the mixed-valence dimer [(dpte)₂Ru^{II}Cl(4,4'-bpy)-Ru^{III}Cl(bpy)₂](PF₆)₃ (417-nm photolysis, 476-nm monitoring beam) using the quencher [*p*-CH₃⁺NC₅H₄C(O)NH₂](PF₆) at 250 K in 40% CH₂Cl₂/60% CH₃CN.

(bpy)₃^{3+/2+*} (Ru(bpy)₃^{3+/(bpy)₂Ru^{III}(bpy⁻)²⁺) has been estimated as -0.81 V using a kinetic quenching approach.²⁰ The potential for the analogous couple in the dimer can be estimated by subtracting the free energy content of the excited state above the ground state from the potential for the ground-state Ru(III)/Ru(II) couple ($E_{1/2} = 0.79\text{ V}$). A reasonable estimate for the excited-state free energy is available from the energy of the emission band (1.78 V), giving $E_{1/2} \approx -0.98\text{ V}$ for both the (bpy)₂ClRu^{II}(L)-based monomeric and dimeric excited-state couples. Given the potentials, oxidative quenching of the MLCT excited states by the pyridinium ion P⁺ is slightly favored thermodynamically:}



The point of the quenching experiments was to use the quenching rate constant data to help to characterize the excited states produced by laser flash photolysis. Because of the sensitivity of k_q on ΔG , k_q values can give, if indirectly, information about excited-state redox potentials. If, for example, k_q values are similar for the series of transients produced by laser flash photolysis of the related series of complexes [(dpte)₂ClRu^{II}(4,4'-bpy)Ru^{II}Cl-

(19) The procedure used in measuring k_q was the emission intensity method described in ref 25 with the only modification being that no added electrolyte was used. The lifetime for [Ru^{II}(bpy)₃]²⁺ used in the Stern-Volmer equation, $I_0/I = 1 + \tau_0 k_q [Q]$, was 788 ns.

(20) Bock, C. R.; Connor, J. A.; Gutierrez, A. R.; Meyer, T. J.; Whitten, D. G.; Sullivan, B. P.; Nagle, J. K. *J. Am. Chem. Soc.* **1979**, *101*, 4815.
 (21) Young, R. C. Ph.D. Dissertation, The University of North Carolina, Chapel Hill, NC, 1977.
 (22) (a) Toma, H. E.; Creutz, C. *Inorg. Chem.* **1979**, *16*, 545. (b) Ballardini, R.; Varani, G.; Idelli, M. T.; Scandola, F.; Balzani, V. *J. Am. Chem. Soc.* **1978**, *100*, 7219.

$(\text{bpy})_2]^{2+}$, $[(\text{dpte})_2\text{ClRu}^{\text{II}}(4,4'\text{-bpy})\text{Ru}^{\text{III}}\text{Cl}(\text{bpy})_2]^{3+}$, and $[(\text{bpy})_2\text{ClRu}^{\text{II}}(4,4'\text{-bpy})]^{2+}$, it would provide strong evidence that the transient states reached by photolysis are closely related. k_q values were obtained by lifetime measurements at a series of quencher concentrations with use of the Stern–Volmer relation

$$1/\tau = 1/\tau_0 + k_q[Q] \quad (3)$$

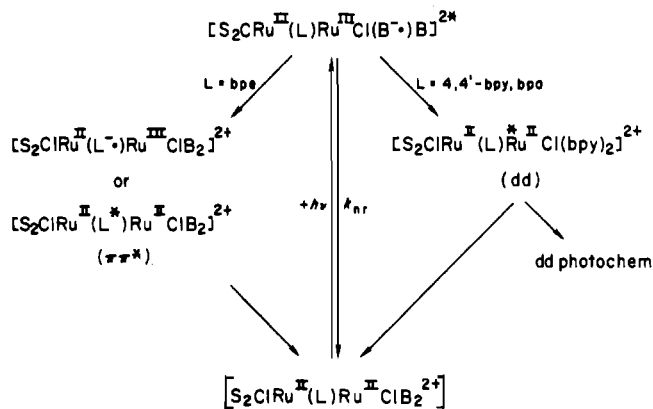
where τ and τ_0 are the measured lifetimes in the presence and absence of quencher and $[Q]$ is the quencher concentration. A plot of $1/\tau$ vs. $[Q]$ is shown in Figure 11, and k_q values are listed in Table V. In order to make detailed comparisons involving the quenching data, it is necessary to make corrections for diffusional effects because quenching rate constants are in the vicinity of the diffusion-controlled limit.^{23,24} This point is discussed in detail elsewhere, where it is estimated that k_d in the solvent mixture used at 250 K and $I = 0$ is $8 \times 10^8 \text{ M}^{-1} \text{ s}^{-1}$.²⁵ The observed quenching rate constants for the series $[(\text{bpy})_2\text{ClRu}^{\text{II}}(4,4'\text{-bpy})]^{2+}$, $[(\text{dpte})_2\text{ClRu}^{\text{II}}(4,4'\text{-bpy})\text{Ru}^{\text{III}}\text{Cl}(\text{bpy})_2]^{3+}$, and $[(\text{dpte})_2\text{ClRu}^{\text{II}}(4,4'\text{-bpy})\text{Ru}^{\text{III}}\text{Cl}(\text{bpy})]^{3+}$ (Table V) are all below this value ($(2.4\text{--}3.6) \times 10^8 \text{ M}^{-1} \text{ s}^{-1}$) and are constant within the rather large error limits involved. The rate constants fall sufficiently below k_d to be in the region of reasonable sensitivity to ΔG , and the similarity in k_q values strongly suggests that the quenching reactions involve closely related excited states.

Discussion

From the evidence provided by transient absorption decay and emission, and absorption spectral measurements, it is evident that the asymmetric dimeric complexes have an extensive excited-state behavior. In order to rationalize the dynamic behavior observed in a systematic and convenient way, it is of value to discuss the results separately for the different types of dimers.

Transient Behavior in the Ru(II)–Ru(II) Dimers. $[(\text{dpte})_2\text{ClRu}^{\text{II}}(\text{L})\text{Ru}^{\text{II}}\text{Cl}(\text{bpy})_2]^{2+}$. The visible absorption spectra of the Ru(II)–Ru(II) dimers are dominated by $\pi^*(\text{bpy}) \leftarrow d\pi$ transitions. Consequently, it is not surprising that photolysis at 457 nm leads to emitting excited states that have the decay characteristics of the related monomer as shown by the data in Table IV for the 4,4'-bpy and bpa dimers. It seems clear that optical excitation in these dimers leads to the sequence of photochemical events that has been established for related monomers: (1) Optical excitation to states largely singlet metal to ligand charge transfer (MLCT) in character, followed by (2) rapid and efficient conversion to states largely triplet in character, which are the emitting states,^{26–32} (3) decay of the ³MLCT states both directly by nonradiative decay to the ground states and indirectly

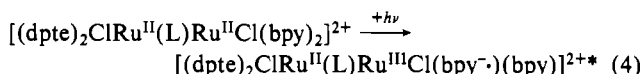
Scheme I



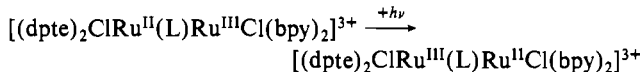
by thermal population of low-lying d dd d states.^{17,34,35} There is clear evidence in the dimers for such d dd d states, namely from the appearance of the expected ligand-loss photoproducts at temperatures near ambient. Other work on related monomers has shown that the two contributions to radiationless decay can be separated by temperature-dependent lifetime studies.^{33–35} Although we did not collect enough data as a function of temperature to separate the two contributions, the slight decrease in τ as a function of temperature from 220 to 280 K for several of the complexes is certainly consistent with the presence of a low-lying dd state or states as shown by the appearance of ligand-loss photochemistry at higher temperatures.

Since the complexes are weak emitters, $\tau = (k_r + k_{nr})^{-1} \approx 1/k_{nr}$ is a direct measure of the nonradiative rate constant. At low temperatures, where the relative contribution to k_{nr} from the dd state is negligible, the transient decay times are controlled by nonradiative decay from the ³MLCT states. When compared to related complexes, the short lifetimes are a direct consequence of the energy gap law and the relatively low ground-state–excited-state energy gap as shown by the data in Table III.^{35,36}

As evidenced by the similarities in lifetimes between related monomers and dimers in Table IV, the picture that emerges for the Ru(II)–Ru(II) dimers with $L = 4,4'\text{-bpy}$ or bpa is that following excitation the usual ³MLCT excited state is formed, decays, and is unaffected by the presence of the second metal site:



This is already an important observation since it suggests the following: (1) Electronic coupling between the two metals is weak. Recall that the same conclusion was reached for the related mixed-valence ions based on the integrated intensities of the IT bands for the transitions



(2) At least at low temperatures, there is no evidence for the intervention of low-lying, dimer-based excited states based on the bridging ligand, e.g. $[(\text{dpte})_2\text{ClRu}^{\text{II}}(\text{L}^-)\text{Ru}^{\text{III}}\text{Cl}(\text{bpy})_2]^{2+*}$, which is not unexpected given the available spectroscopic information from MLCT absorption spectra.^{4,8,9,13,16}

However, the situation may be different for the bpe dimer, $[(\text{dpte})_2\text{ClRu}^{\text{II}}(\text{bpe})\text{Ru}^{\text{II}}\text{Cl}(\text{bpy})_2]^{2+}$, where the lifetime of the dimer is shorter by a factor of 2.5 than that of the monomer,

- (23) Noyes, R. M. *Prog. React. Kinet.* **1961**, *1*, 129.
 (24) (a) Debye, P. *Trans. Faraday Soc.* **1942**, *82*, 265. (b) von Smolouchowski, M. Z. *Phys. Chem. (Leipzig)* **1917**, *92*, 129. (c) Petrucci, S. "Ionic Interactions"; Academic Press: New York, NY 1971; Vol. II, pp 101–109. (d) Hemnes, P. J. *Am. Chem. Soc.* **1972**, *94*, 75.
 (25) Curtis, J. C. Ph.D. Dissertation, The University of North Carolina, Chapel Hill, NC, 1980.
 (26) (a) Hager, G. D.; Crosby, G. A. *J. Am. Chem. Soc.* **1975**, *97*, 7031. (b) Hager, G. D.; Watts, R. J.; Crosby, G. A. *J. Am. Chem. Soc.* **1975**, *97*, 7037. (c) Demas, J. N.; Crosby, G. A. *J. Am. Chem. Soc.* **1971**, *93*, 2841.
 (27) (a) Ferguson, J.; Kraus, E. R. *Chem. Phys. Lett.* **1982**, *93*, 21. (b) Ferguson, J.; Herren, F.; McLaughlin, G. M. *Chem. Phys. Lett.* **1982**, *84*, 376. (c) Ferguson, J.; Herren, F. *Chem. Phys. Lett.* **1982**, *89*, 371.
 (28) (a) Felix, F.; Ferguson, J.; Gudel, H. J.; Ludi, A. *J. Am. Chem. Soc.* **1980**, *102*, 4096. (b) Descourtins, S.; Felix, F.; Ferguson, J.; Gudel, H. J.; Ludi, A. *J. Am. Chem. Soc.* **1980**, *102*, 4102. (c) Felix, F.; Ferguson, J.; Gudel, H. J.; Ludi, A. *Chem. Phys. Lett.* **1979**, *62*, 153.
 (29) (a) Bradley, P. G.; Kress, N.; Hornberger, B. A.; Dallinger, R. F.; Woodruff, W. H. *J. Am. Chem. Soc.* **1981**, *103*, 744. (b) Dallinger, R. F.; Woodruff, W. H. *J. Am. Chem. Soc.* **1979**, *101*, 4391.
 (30) (a) Carlin, C. M.; DeArmond, M. K. *Chem. Phys. Lett.* **1982**, *89*, 297. (b) DeArmond, M. K.; Carlin, C. M.; Huang, W. L. *Inorg. Chem.* **1980**, *19*, 62.
 (31) Kober, E. M.; Meyer, T. J. *Inorg. Chem.* **1982**, *21*, 3967.
 (32) Kober, E. M.; Meyer, T. J. *Inorg. Chem.*, in press.
 (33) Allsopp, S. R.; Cox, A.; Kemp, T. J.; Reed, J. *Chem. Soc., Faraday Trans. 1*, **1978**, *74*, 1275.

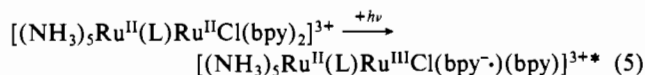
- (34) (a) Van Houten, J.; Watts, R. J. *Inorg. Chem.* **1978**, *17*, 3381. (b) Van Houten, J.; Watts, R. J. *Am. Chem. Soc.* **1976**, *98*, 4853.
 (35) (a) Caspar, J. V.; Meyer, T. J. *J. Am. Chem. Soc.* **1983**, *105*, 5583–5590. (b) Caspar, J. V.; Meyer, T. J. *Inorg. Chem.* **1983**, *22*, 2444–2453. (c) White, R.; Rillema, D. P.; Allen, G. H.; Meyer, T. J. *J. Am. Chem. Soc.* **1984**, *23*, 2613.
 (36) (a) Caspar, J. V.; Kober, E. M.; Sullivan, B. P.; Meyer, T. J. *J. Am. Chem. Soc.* **1982**, *104*, 630. (b) Caspar, J. V.; Sullivan, B. P.; Kober, E. M.; Meyer, T. J. *Chem. Phys. Lett.*, **1982**, *91*, 91. (c) Caspar, J. V.; Meyer, T. J. *J. Phys. Chem.* **1983**, *87*, 952.

$[(bpy)_2ClRu(bpe)]^+$. For the bpe dimer the decrease in lifetime and loss of temperature dependence in τ may be attributable to population and decay from a lower lying, bridging ligand-based MLCT state, $[(dpte)_2ClRu^{II}(bpe^-)Ru^{III}Cl(bpy)_2]^{3+}$, or from a $\pi\pi^*$ state localized on bpe, $[(dpte)_2ClRu^{II}(bpe^*)Ru^{III}Cl(bpy)_2]^{2+}$. Note that the lowest π^* level is lower for bpe than for the other two bridging ligands; e.g., the $\pi^*(L) \leftarrow d\pi(Ru^{II}Cl(dpte)_2)$ transition in the monomers $(dpte)_2ClRu(L)^+$ comes at 394 nm for $L = bpe$ and at 376 nm for $L = 4,4'$ -bpy. The equivalent transitions in the dimers are expected to be masked by $\pi^*(bpy) \leftarrow Ru^{II}$ bands but to be on the low-energy side of the bpy-based manifold. Consequently, it would not be surprising if the lowest thermally equilibrated, bpe-based MLCT state lies near or even below the lowest bpy-based MLCT state.

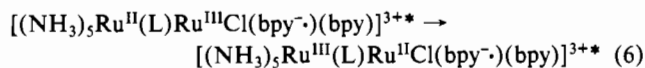
The photophysical events for which there is evidence following visible photolysis of the Ru(II)–Ru(II) dimers are summarized in the Jablonski-type diagram in Scheme I. In Scheme I and later schemes the disulfur ligands $PhSCH_2CH_2SPh$ are abbreviated as S and 2,2'-bipyridine as B.

Ru(II)–Ru(II) Dimers. $[(NH_3)_5Ru^{II}(L)Ru^{II}Cl(bpy)_2]^{3+}$. For the dimers $[(NH_3)_5Ru^{II}(L)Ru^{II}Cl(bpy)_2]^{3+}$ with $L = 4,4'$ -bpy or bpe, the absorption spectra and excited-state manifold are complicated by the appearance of relatively low-lying $\pi^*(L) \leftarrow d\pi(-Ru^{II}(NH_3)_5)$ states. For example, for the dimer $[(NH_3)_5Ru^{II}(bpe)Ru^{II}Cl(bpy)_2]^{3+}$ a new, intense band at 507 nm ($\epsilon = 2.21 \times 10^4$) appears when compared to the spectrum of $[(dpte)_2ClRu^{II}(bpe)Ru^{II}Cl(bpy)_2]^{2+}$. Even following laser flash photolysis at 452 nm, where absorption is dominated by $\pi^*(bpy) \leftarrow d\pi(Ru^{II})$ based chromophores, no transient absorbance changes are observed and the characteristic bpy-based 3MLCT emission is quenched. With $L = bpa$, the transient absorbance and emission properties of the dimer are within experimental error those of the monomer $[(bpy)_2ClRu(bpa)]^+$. There is no guarantee that the relative ordering of MLCT levels will carry over from the largely singlet states observed in absorption to the largely triplet states which are, no doubt, ultimately populated following photolysis, but it seems reasonable that they should.

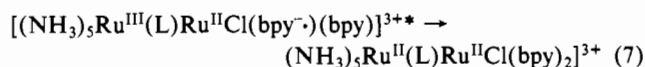
Following excitation to give the bpy-based 3MLCT states



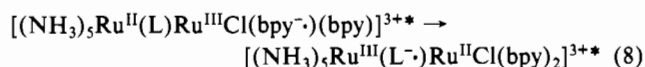
quenching could occur by intramolecular, reductive electron-transfer quenching



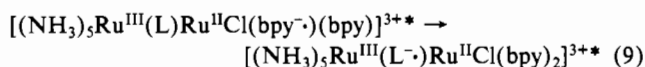
followed by nonradiative decay of the "remote" MLCT state



Alternatively, quenching of the Ru–bpy MLCT state may occur by energy transfer to the lower $\pi^*(L) \leftarrow d\pi(-Ru^{II}(NH_3)_5)$ states

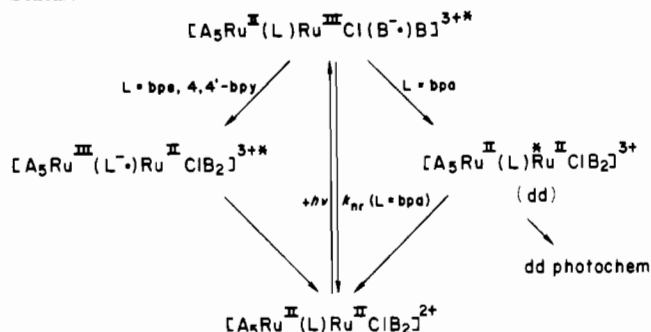


The energy-transfer product could also arise from two successive one-electron-transfer steps, reductive quenching (eq 6) followed by ligand–ligand electron transfer:



From reduction potentials for the $(NH_3)_5Ru^{III/II}(L^-)$ (0.35–0.43 V) and excited-state $-(L)Ru^{III/II}Cl(bpy^-)(bpy)$ couples (0.3 V), the latter estimated from the emission energy of ~ 700 nm (14300 cm^{-1}) and ground-state $Ru^{III/II}$ potentials in Table IV, the reductive quenching step is nearly spontaneous. Nonetheless, given the observation of facile intramolecular energy transfer in related dimers, the energy-transfer possibility is more appealing. It is also consistent with the lack of quenching in the bpa-bridged dimer, where the $\pi^*(L) \leftarrow d\pi(-Ru^{II}(NH_3)_5)$ levels appear to lie above

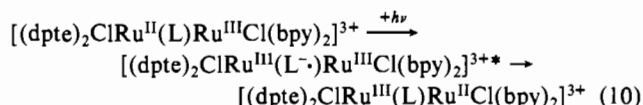
Scheme II



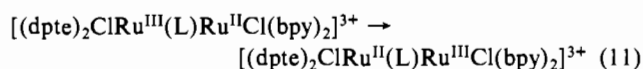
the 3MLCT -bpy manifold and the lifetime of the 3MLCT bpy-based luminophore is relatively unchanged in the dimer. From earlier work on transient behavior in $-Ru^{II}(NH_3)_5$ -based MLCT states¹⁸ and our observation of a short-lived ($\tau < 2$ ns) transient following photolysis of $[(NH_3)_5Ru^{II}(4,4'$ -bpy)]²⁺, once formed by energy transfer, the lower lying $-Ru^{II}(NH_3)_5$ MLCT states are expected to decay rapidly to the ground state.

Following the lead of the previous section, the likely photophysical processes that occur following photolysis of the pentaammine dimers are shown in Scheme II, where A is used as an abbreviation for the ammine ligand.

Ru(II)–Ru(III) Dimers. $[(dpte)_2ClRu^{II}(L)Ru^{III}Cl(bpy)_2]^{3+}$. Our major interest was in the photophysical properties of the mixed-valence dimers. Oxidation of the Ru(II)–Ru(II) dimers occurs at the Ru–bpy, site resulting in the loss of the $\pi^*(bpy) \leftarrow d\pi(Ru^{II})$ chromophore. One thought was that, following excitation, a series of sequential steps such as

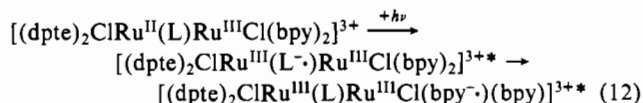


would occur, giving the high-energy-oxidation-state isomer of the mixed-valence dimers. If so, the possibility would exist for obtaining a direct measurement of the rate constant for intramolecular electron transfer by observing the relaxation of the higher energy isomer.¹⁸

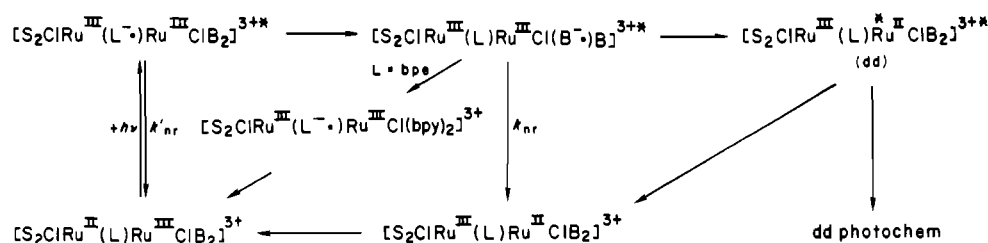


The transient absorbance events that occur in the mixed-valence dimers were induced by excitation at 417 nm. In this spectral range optical absorption is dominated by MLCT transitions involving the bridging ligand, $(dpte)_2ClRu^{II}(L^-) \xrightarrow{+h\nu} (dpte)_2ClRu^{III}(L^-)$, and LMCT transitions localized at the oxidized $-Ru^{III}Cl(bpy)_2$ site. Following excitation of the Ru(I)–Ru(III) dimers, the remarkable observation was made that the resulting emission and transient decay characteristics are those of the Ru^{II} -bpy site even though the site is in oxidation state III initially. Further confirmation of the nature of the excited state where $L = 4,4'$ -bipyridine comes from the results of the oxidative-quenching experiments in Table V. From those results, the excited state reached in the Ru(II)–Ru(III) dimer must have nearly the same redox potential as a reducing agent as the Ru(bpy) MLCT states of the monomer $(bpy)_2ClRu(4,4'$ -bpy)⁺ and the Ru(II)–Ru(II) dimer $[(dpte)_2ClRu(4,4'$ -bpy)Ru^{II}Cl(bpy)₂]²⁺.

The available evidence clearly points to the appearance of the bpy-based 3MLCT state $-(L)Ru^{III}Cl(bpy^-)(bpy)$ following excitation even though the corresponding chromophore does not exist in the Ru(II)–Ru(III) dimers. The most reasonable explanation for the appearance of this state is via initial Ru(II) $\rightarrow \pi^*(L)$ excitation followed by intramolecular, ligand to ligand electron transfer:



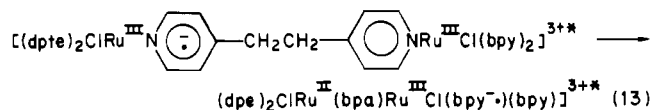
Scheme III



It seems unlikely that excitation of the LMCT-based chromophore at $-(L)Ru^{III}Cl(bpy)_2$ followed by intramolecular energy transfer represents a significant pathway for population of the bpy-based 3MLCT state. Given the electronic nature of such states, e.g. Ru^{II}, Cl , they are expected to have large Franck-Condon contributions to their energies and to relax rapidly to energies below the 3MLCT states.

The appearance and subsequent decay of the 3MLCT -bpy state represents a "hold back" which prevents the observation of "relaxation" from the mixed-valence oxidation-state isomer. From the lifetime data in Table IV, it can be estimated that $k(220\text{ K}) > 10^7\text{ s}^{-1}$ for intramolecular electron transfer (eq 11) in all three dimers. With use of the properties of the IT bands for the dimers and the Hush equations mentioned earlier, it can be estimated that $k \approx 6 \times 10^{10}$, and it is not surprising that the experiment was unsuccessful. It should be noted that application of the Hush equation to these dimers is an approximation since it treats the contributions from Ru-Cl trapping vibrations classically and there are, no doubt, multiple components to the IT bands arising from the existence of low-lying spin-orbit states at Ru(III).³⁷

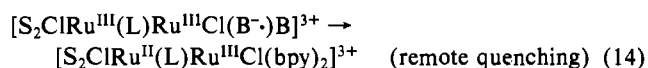
There are two additional effects worth noting that appear for the mixed-valence dimers with $L = bpe, bpa$. For the bpe-bridged dimer $[(dpte)_2ClRu^{II}(bpe)Ru^{III}Cl(bpy)_2]^{3+}$ the 3MLCT -bpy lifetime at 220 K is decreased by a factor of ~ 2 compared to that of the monomer $[(bpy)_2ClRu^{II}(bpe)]^+$. As in the Ru(II)-Ru(II) dimer, this decrease may signal the onset of a contribution to nonradiative decay arising from population and subsequent decay of a bpe-based state. Since the bpe-based MLCT state $[(dpte)_2ClRu^{III}(bpe^-)Ru^{III}Cl(bpy)_2]^{3+}$ is the initial high-energy state formed by excitation, in this case the lower energy bpe-based state must be $\pi\pi^*(bpe)$ in character. For the bpa-bridged dimer $[(dpte)_2ClRu^{II}(bpa)Ru^{III}Cl(bpy)_2]^{3+}$ the transient decay is identical with that for the corresponding monomer, but both the extent of the absorbance change and the noticeably weakened emission suggest that the ligand to ligand electron-transfer step in eq 12 may be in competition with decay from the initially populated, bpa-localized MLCT excited state, eq 13.



That the bpy-based 3MLCT state is observed at all is interesting since it requires that ligand to ligand electron transfer occur through the saturated portion of the ligand or by direct, through-space outer-sphere overlap between the electron donor and acceptor sites.

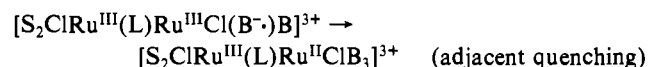
The apparent photophysical events that occur following photolysis of the mixed-valence dimers is summarized in Scheme III, where, once again, the disulfur ligands are abbreviated as S and 2,2'-bipyridine as B.

In the context of Scheme III there are two additional points to consider. The first is the *absence* of remote intramolecular Ru-bpy MLCT quenching by $(dpte)_2ClRu^{III}$:



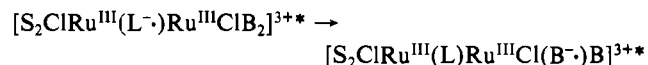
(37) Kober, E. M.; Goldsby, K. A.; Narayana, D. N. S.; Meyer, T. J. *J. Am. Chem. Soc.* **1983**, *105*, 4303.

Such an intramolecular quenching step is in competition with the usual Ru-bpy-based decay:

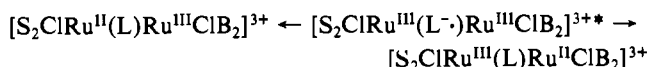


Interestingly, remote quenching by Ru(III) gives the stable mixed-valence isomer directly and is actually the *preferred* process energetically. The apparent preference of "adjacent" over "remote" quenching by Ru(III) can be reconciled on the basis of the principles of radiationless decay theory.³⁸ Both quenching paths are nonradiative excited-state decay processes, and their rate constants are expected to *decrease as ΔE becomes more favorable* as predicted by the energy gap law.³⁸ More importantly, non-radiative decay rate constants also depend on vibrationally induced electronic coupling through terms of the form $C_k^2 = \langle \Psi_g | \partial / \partial Q_k | \Psi_e \rangle^2$, where Ψ_e and Ψ_g are the excited- and ground-state electronic wave functions. Q_k is the coordinate for a particular normal mode (promoting mode) of the system, which when varied has the effect of mixing the electronic wave functions. Given the nature of the electron transfers involved, the magnitude of C_k^2 is expected to be considerably greater for the adjacent Ru(III) site where a series of metal-ligand bends and stretches are available to serve as promoting modes.³⁹

The energy gap law argument is particularly helpful in understanding why ligand to ligand electron transfer



which leads to the emitting 3MLCT -bpy state, can compete effectively with nonradiative decay processes where the excited electron returns to one of the two Ru(III) sites:



Although the nonradiative processes are highly favored energetically, their rate constants are dictated by the energy gap law. $k \propto \exp|\Delta E|$, and k is expected to *decrease* as ΔE becomes more favorable. For the ligand to ligand electron-transfer reaction, the electron-transfer process occurs in the "normal" region. In this region, in the classical limit, $k \propto \exp[(\chi + \Delta E)^2 / 4\chi k_B T]$ and k is expected to *increase* as ΔE becomes more favorable. $\chi/4$ is the classical vibrational trapping energy arising from intramolecular and solvent vibrations. An additional feature of importance in the normal region is the extent of electronic coupling between the electron donor and acceptor sites either through space or by mixing with orbitals at the Ru(III) site. It should be noted that there are clear precedences for the ligand to ligand electron-transfer reaction proposed here based on transient studies on

(38) (a) Freed, K. F.; Jortner, J. *J. Chem. Phys.* **1970**, *52*, 6272. (b) Englman, R.; Jortner, J. *Mol. Phys.* **1970**, *18*, 145. (c) Lin, S. H. *J. Chem. Phys.* **1966**, *44*, 3759.

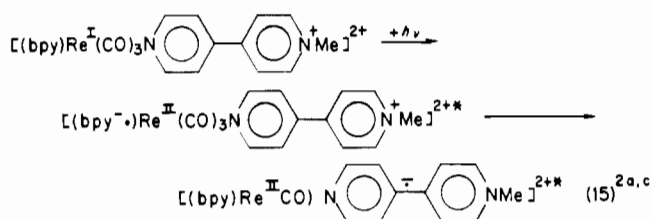
(39) Kober, E. M. Ph.D. Dissertation, The University of North Carolina, Chapel Hill, NC, 1982.

(40) Sullivan, B. P.; Abruna, H.; Finklea, H. O.; Salmon, D. J.; Nagle, J. K.; Meyer, T. J.; Sprintschnik, H. *Chem. Phys. Lett.* **1978**, *58*, 389.

(41) Westmoreland, T. D.; Le Bozec, H.; Murray, T. W.; Meyer, T. J. *J. Am. Chem. Soc.*, in press.

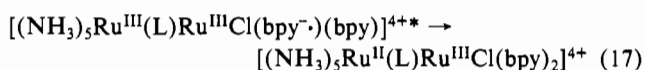
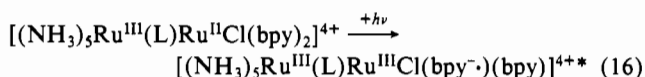
(42) (a) Meyer, T. J. *Prog. Inorg. Chem.* **1983**, *30*, 389. (b) Meyer, T. J. In "Inorganic Chemistry: Toward the 21st Century"; Chisholm, M. H., Ed.; American Chemical Society: Washington, DC, ACS Symp. Ser. No. 211, p 157.

intramolecular chromophore–quencher complexes, e.g.



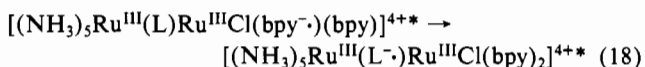
$[(\text{NH}_3)_5\text{Ru}^{\text{III}}(\text{L})\text{Ru}^{\text{II}}\text{Cl}(\text{bpy})_2]^{4+}$. The situation with regard to the mixed-valence dimers containing the $(\text{NH}_3)_5\text{Ru}^{\text{III}}(\text{L})-$ group is quite different. Here the effect of the ligand-induced variations in the Ru(III/II) couples is such that the site of oxidation in the Ru(II)–Ru(II) dimers is at the pentaammine site and the $\pi^*(\text{bpy}) \leftarrow d\pi(\text{Ru}^{\text{II}})$ chromophore is maintained in the mixed-valence dimer. Laser flash photolysis into the MLCT chromophore (at 457 nm) results in the observation of, at best, a weak, rapid transient bleaching and no observable emission for $\text{L} = \text{bpe}$ or $4,4'$ -bpy. On the other hand, for the dimer with $\text{L} = \text{bpa}$, both a noticeable emission and a transient bleaching with τ_0 within experimental error of that for the monomer $[(\text{bpy})_2\text{ClRu}(\text{bpa})]^{4+}$ are observed (Tables III and IV).

Although we have no clear evidence on the point, there are at least two reasonable pathways that can explain the loss of observable transient behavior in the dimers on our time scale. The first is by intramolecular oxidative quenching of the ${}^3\text{MLCT}$ -bpy excited state

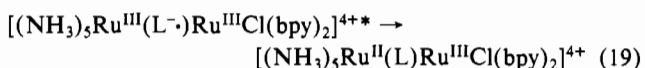


which is expected to be less favored over the equivalent process in the dpte -based dimer (eq 14). There may also be more favorable Franck–Condon, vibrational overlap factors associated with excited-state nonradiative processes at the pentaammine site.

The second possibility is via ligand to ligand electron transfer to give bridging ligand-based MLCT states



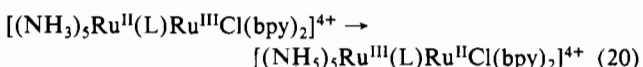
followed by their decay



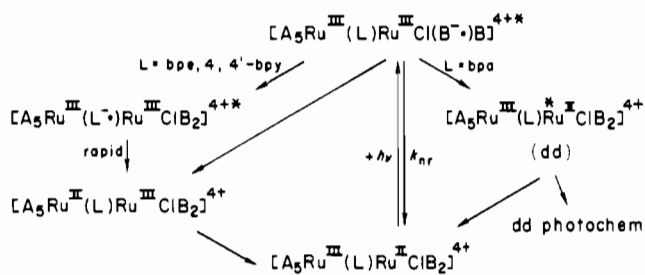
which is expected to be rapid given the short lifetimes of other $\pi^*(\text{L})-d\pi(\text{Ru}^{\text{II}}(\text{NH}_3)_5)$ -based excited states. Callahan has shown that, in the dimers $[(\text{NH}_3)_5\text{Ru}^{\text{III}}(\text{L})\text{Ru}^{\text{II}}\text{Cl}(\text{bpy})_2]^{4+}/^{3+}$, the $\pi^*(\text{L}) \leftarrow d\pi(\text{Ru}^{\text{II}}\text{Cl}(\text{bpy})_2)$ and $\pi^*(\text{bpy}) \leftarrow d\pi(\text{Ru}^{\text{II}}\text{Cl}(\text{bpy})_2)$ transitions are located in the same energy region, suggesting that the energy change associated with the ligand–ligand electron-transfer reaction in eq 19 may be favorable.⁴

The fact that the ${}^3\text{MLCT}$ -bpy excited state appears to be relatively unaffected by the remote $(\text{NH}_3)_5\text{Ru}^{\text{III}}-$ group in the bpa dimer is consistent with the operation of either quenching pathway. For the bpa -bridged dimer the L-based MLCT states are at considerably higher energy, thus eliminating eq 18 as a quenching pathway. Even though the appearance of IT bands in related dimers suggests that weak electronic coupling exists between Ru^{II} and Ru^{III} sites in $\text{Ru}^{\text{III}}(\text{bpa})\text{Ru}^{\text{II}}$ dimers, vibrationally induced electronic coupling through the unit $\text{Ru}^{\text{III}}(\text{L})\text{Ru}^{\text{III}}(\text{bpy}^{\cdot-})$, which is necessary for remote excited-state quenching, may be relatively insignificant.

In either case the mixed-valence pentaammine dimers are of interest in the context of the original goal of observing relaxation from a high-energy, mixed-valence dimer



Scheme IV



Because the relaxation pathways leading to the high-energy oxidation-state dimer (eq 19) are relatively facile, it is conceivable that picosecond experiments would allow for the direct observation of the relaxation process in eq 20. From the properties of the IT band we estimate that $k \approx 5 \times 10^9 \text{ s}^{-1}$ ($\tau \approx 200 \text{ ps}$) for intramolecular electron transfer in the $4,4'$ -bpy-bridged dimer.

The probable sequence of events following excitation of the MLCT-bpy chromophore in the mixed-valence pentaammine dimers is shown in Scheme IV, where A is NH_3 .

Final Comments. One of the real values to emerge from this work is the continued evolution of the factors at the molecular level that are needed to control the directional sense of charge transport in complex molecules. For chemically linked chromophores or in chromophore–quencher complexes, it is important to establish the “rules” that determine the possible direct migration of energy or electrons following initial excitation at a chromophoric site. The results described here provide insight in the following sense:

(1) The basis for the dominant chromophore in Ru–Ru dimers can be controlled by varying ligand environments and electron content, e.g., compare $[(\text{dpte})_2\text{ClRu}^{\text{II}}(\text{L})\text{Ru}^{\text{II}}\text{Cl}(\text{bpy})_2]^{2+}$, $[(\text{dpte})_2\text{ClRu}^{\text{II}}(\text{L})\text{Ru}^{\text{III}}\text{Cl}(\text{bpy})_2]^{3+}$, and $[(\text{NH}_3)_5\text{Ru}^{\text{III}}(\text{L})\text{Ru}^{\text{II}}\text{Cl}(\text{bpy})_2]^{4+}$.

(2) If appropriate energetic and electronic coupling terms are favorable, initial excitation can be followed by facile energy, e.g., $[(\text{NH}_3)_5\text{Ru}^{\text{III}}(\text{L})\text{Ru}^{\text{III}}\text{Cl}(4,4'\text{-bpy}^{\cdot-})(\text{bpy})]^{3+*} \rightarrow [(\text{NH}_3)_5\text{Ru}^{\text{III}}(\text{L}^{\cdot-})\text{Ru}^{\text{II}}\text{Cl}(\text{bpy})_2]^{3+*}$, or electron transfer, $[(\text{dpte})_2\text{ClRu}^{\text{III}}(\text{L}^{\cdot-})\text{Ru}^{\text{II}}\text{Cl}(\text{bpy})_2]^{3+*} \rightarrow [(\text{dpte})_2\text{ClRu}^{\text{III}}(\text{L})\text{Ru}^{\text{II}}\text{Cl}(\text{bpy}^{\cdot-})(\text{bpy})]^{3+*}$, to remote sites in the molecule.

(3) The pattern of electron-transfer events following the initial excitation in mixed-valence dimers is determined by competitive ligand to ligand, e.g., $[(\text{dpte})_2\text{ClRu}^{\text{III}}(\text{L}^{\cdot-})\text{Ru}^{\text{III}}\text{Cl}(\text{bpy})_2]^{3+*} \rightarrow [(\text{dpte})_2\text{ClRu}^{\text{II}}(\text{L})\text{Ru}^{\text{III}}\text{Cl}(\text{bpy}^{\cdot-})(\text{bpy})_2]^{3+}$ and ligand to metal electron transfer, e.g., $[(\text{dpte})_2\text{ClRu}^{\text{III}}(\text{L}^{\cdot-})\text{Ru}^{\text{III}}\text{Cl}(\text{bpy})_2]^{3+*} \rightarrow [(\text{dpte})_2\text{ClRu}^{\text{II}}(\text{L})\text{Ru}^{\text{III}}\text{Cl}(\text{bpy})_2]^{3+}$. Ligand to ligand electron transfer leads to a direct charge transfer and ligand to metal electron transfer to excited-state decay. Of the two processes, ligand to ligand electron transfer is a process in the “normal” region and ligand to metal electron transfer is an excited-state, nonradiative decay. The decay characteristics of the two processes have different dependences on such innate molecular features as ΔE and vibrational overlaps and should be controllable in a relative sense by varying such factors as temperature, the extent of vibrational trapping (χ) through the degree of excited-state distortion, and ΔE .

(4) Because of the energy gap law dependence on ΔE , excited-state decay via ligand to metal electron transfer is surprisingly slow, allowing ligand to ligand electron transfer to compete.

(5) Remote quencher sites may not be effective in excited-state quenching, e.g., in $[(\text{dpte})_2\text{ClRu}^{\text{III}}(\text{L})\text{Ru}^{\text{III}}\text{Cl}(\text{bpy}^{\cdot-})(\text{bpy})]^{3+*}$, either or both because of energy gap law considerations and because of insignificant vibrationally induced electronic coupling.

Acknowledgments are made to the National Science Foundation under Grant CHE-8008922 and to the Army Research Office—Durham under Grant DAAG29-82-K-0111 for support of this research.

Registry No. $[(\text{NH}_3)_5\text{Ru}^{\text{II}}(4,4'\text{-bpy})\text{Ru}^{\text{II}}\text{Cl}(\text{bpy})_2](\text{PF}_6)_3$, 94070-01-6; $[(\text{NH}_3)_5\text{Ru}^{\text{III}}(4,4'\text{-bpy})\text{Ru}^{\text{II}}\text{Cl}(\text{bpy})_2](\text{PF}_6)_4$, 94070-03-8; $[(\text{NH}_3)_5\text{Ru}^{\text{II}}(\text{bpe})\text{Ru}^{\text{II}}\text{Cl}(\text{bpy})_2](\text{PF}_6)_3$, 54713-86-9; $[(\text{NH}_3)_5\text{Ru}^{\text{III}}(\text{bpe})\text{Ru}^{\text{II}}\text{Cl}(\text{bpy})_2](\text{PF}_6)_3$, 54713-86-9.

(bpy)₂](PF₆)₄, 94070-05-0; [(NH₃)₅Ru^{II}(bpa)Ru^{II}Cl(bpy)₂](PF₆)₃, 94070-06-1; [(NH₃)₅Ru^{III}(bpa)Ru^{II}Cl(bpy)₂](PF₆)₄, 94070-08-3; [(dpte)₂ClRu^{II}(4,4'-bpy)Ru^{II}Cl(bpy)₂](PF₆)₂, 94070-09-4; [(dpte)₂ClRu^{II}(4,4'-bpy)Ru^{III}Cl(bpy)₂](PF₆)₃, 94070-11-8; [(dpte)₂Ru^{II}Cl(bpe)Ru^{II}Cl(bpy)₂](PF₆)₂, 94132-58-8; [(dpte)₂ClRu^{II}(bpe)Ru^{III}Cl(bpy)₂](PF₆)₃, 94070-13-0; [(dpte)₂ClRu^{II}(bpa)Ru^{II}Cl(bpy)₂](PF₆)₂, 94070-14-1; [(dpte)₂ClRu^{II}(bpa)Ru^{III}Cl(bpy)₂](PF₆)₃, 94070-16-3; [(bpy)₂Ru^{II}Cl(4,4'-bpy)](PF₆)₂, 49734-36-3; [(bpy)₂Ru^{II}Cl(bpe)](PF₆)₂, 49734-42-1; [(bpy)₂Ru^{II}Cl(bpa)](PF₆)₂, 54713-80-3; [(NH₃)₅Ru^{II}(4,4'-bpy)](PF₆)₂, 94070-17-4;

[(dpte)₂Ru^{II}Cl(4,4'-bpy)](PF₆)₂, 94070-19-6; [(dpte)₂ClRu^{II}(bpe)](PF₆)₂, 94070-21-0; [(dpte)₂ClRu^{II}(bpa)](PF₆)₂, 94070-23-2; [(NH₃)₅Ru^{II}(bpe)](PF₆)₂, 94070-24-3; [(NH₃)₅Ru^{II}(bpa)](PF₆)₂, 54713-94-9; *trans*-[(dpte)₂Ru^{II}Cl₂], 32648-33-2; [(dpte)₂ClRu^{II}(NCCH₃)](PF₆)₂, 94070-26-5; dpte, 622-20-8; *p*-CH₃⁺NC₅H₄CONH₂, 45791-94-4.

Supplementary Material Available: Tables of elemental analysis data and UV-visible absorption maxima and extinction coefficients for the compounds used in the study (6 pages). Ordering information is given on any current masthead page.

Contribution from the William Rand Kenan, Jr. Laboratories of Chemistry, The University of North Carolina at Chapel Hill, Chapel Hill, North Carolina 27514

Fast Atom Bombardment and Field Desorption Mass Spectrometry of Organometallic Derivatives of Ruthenium(II) and Osmium(II)

RONALD L. CERNY, B. PATRICK SULLIVAN, MAURICE M. BURSEY,* and THOMAS J. MEYER

Received November 2, 1983

The fast atom bombardment (FAB) and field desorption (FD) mass spectrometric analysis of 18 involatile, cationic organometallic derivatives of 2,2'-bipyridine (bpy) complexes of Ru(II) and Os(II) containing η^2 -alkene, η^2 -alkyne, carbonyl, alkyl, and hydrido ligands is presented. Field desorption (FD) and fast atom bombardment (FAB) mass spectrometry are used in concert. In the area of (polypyridyl)metal complex chemistry, these techniques are powerful structural tools; the former gives information on the intact cation, and the latter, fragmentations characteristic of the ligands. The fragmentations can be interpreted on a chemical basis by invoking four concepts: redox fragmentation of metal-ligand bonds, i.e., homolytic dissociation; the simple loss of neutral ligands, depending upon their thermal lability; intramolecular, oxidative addition of coordinated bpy; reductive elimination of HX (X = Cl, H, alkyl).

Introduction

The use of new mass spectrometric techniques as tools for the characterization of organometallic complexes of low volatility has developed rapidly during the last several years. Specifically, field desorption (FD) mass spectrometry¹⁻⁴ has been applied in a variety of studies to yield parent ion molecular weight data, although in most instances very little fragment ion information is obtained. Fast atom bombardment (FAB) mass spectrometry,^{5,6} although only applied in a few cases, promises to be extremely valuable: parent ion and fragmentation data are exhibited for most samples.⁷⁻¹⁰ One of the challenges to be met in utilizing FAB is to relate the fragmentation patterns produced to the structures of the unknown organometallic complex, i.e., to identify the major fragmentation pathways. Given our recent success in applying FAB to a series of coordination complexes and in interpreting the fragment ions in terms of the complexes' thermal chemistry, an obvious extension is to organometallic complexes.

In this paper we present primarily FAB spectral studies but, where appropriate, give complementary FD data, for a series of 2,2'-bipyridine (bpy) organometallic derivatives of Os(II) and Ru(II). The organometallic moieties in our studies are η^2 -alkene, η^2 -alkyne, η^6 -benzene, η^5 -cyclopentadienyl, carbonyl, alkyl, and hydride ligands.

The results presented here are extremely encouraging with regard to the use of these spectroscopies in a complementary fashion for characterization of the molecular weight (parent ion mass) of unknown involatile organometallic species, especially cations. Generally, when FAB was unable to provide parent ion information, FD was able to do so. In addition, we will demonstrate that the FAB fragmentation patterns can be interpreted by a combination of simple bond-cleavage processes and redox events.

Experimental Section

Instrumentation. Field Desorption. A Du Pont 21-492B mass spectrometer modified for field desorption was used in this study. The instrument was operated at a 3-kV accelerating potential, and the cathode was held at -7 kV. Samples were dissolved in methylene chloride and placed on the emitter dendrites by the dipping method. Cobalt dendrites were used; their preparations have been described elsewhere.¹¹ Heating currents of 15-30 mA were sufficient to desorb the samples. The source was maintained at ambient temperature.

Fast Atom Bombardment. A VG 7070 mass spectrometer equipped with a standard VG data system was used in the FAB experiments. The instrument was fitted with a modified saddle field ion source obtained from Ion Tech Ltd. to serve as the atom beam gun. Xenon was used to produce the primary beam. A primary current of 1 mA at an energy of 4-8 KeV provided good sample ion intensities. A stainless-steel probe tip was covered with a small piece of aluminum foil to provide a clean surface for each sample. The sample was placed onto the foil as either a solution or suspension in glycerol. In cases where low solubility in this glycerol matrix seemed to result in poor spectral quality, the sample was first dissolved in a small amount of dimethylformamide. This solution was then placed on the probe with a small amount of glycerol. This enabled us to obtain spectra of previously intractable complexes.

Samples. The carbonyl complexes [Ru(bpy)₂(CO)X](PF₆) (X = H, Cl) and [Os(bpy)₂(CO)X](PF₆) (X = H, Cl, CF₃, CF₃CO₂) were prepared by published techniques.¹² The synthesis of the complex Ru(η^2 -C₅H₅)(bpy)Cl will be described in a forthcoming publication.¹³ The

- Beckey, H. D. *Int. J. Mass Spectrom. Ion Phys.* **1969**, *2*, 500-503.
- Games, D. E.; Gower, J. L.; Gower, M.; Kane-Maguire, L. A. P. *J. Organomet. Chem.* **1980**, *193*, 229-234.
- Games, D. E.; Gower, J. L.; Kane-Maguire, L. A. *J. Chem. Soc., Dalton Trans.* **1981**, 1994-1996.
- McEwen, C. N.; Ittel, S. D. *Org. Mass Spectrom.* **1980**, *15*, 35-37.
- Barber, M.; Bordoli, R. S.; Sedgwick, R. D.; Tyler, A. N. *J. Chem. Soc., Chem. Commun.* **1981**, 345-327.
- Barber, M.; Bordoli, R. S.; Sedgwick, R. D.; Tyler, A. N. *Nature (London)* **1981**, *293*, 270-275.
- Tkatchenko, I.; Neibecker, D.; Fraisse, D.; Gomez, F.; Barofsky, D. F. *Int. J. Mass Spectrom. Ion Phys.* **1983**, *46*, 499-502.
- Johnstone, R. A. W.; Lewis, I. A. S. *Int. J. Mass Spectrom. Ion Phys.* **1983**, *46*, 451-454.
- Barber, M.; Bordoli, R. S.; Sedgwick, R. D.; Tyler, A. N. *Biomed. Mass Spectrom.* **1981**, *18*, 491-495.
- Miller, J. M. *J. Organomet. Chem.* **1983**, *249*, 299-302.

- Burse, M. M.; Rechsteiner, C. E., Jr.; Youngless, T. L.; Fraley, D. F.; Sammons, M. C.; Hass, J. R. *Adv. Mass Spectrom.* **1978**, *7*, 932-938.
- (a) Caspar, J. V.; Sullivan, B. P.; Meyer, T. J. *Organometallics* **1983**, *2*, 551-554. (b) Sullivan, B. P.; Caspar, J. V.; Johnson, S. R.; Meyer, T. J. *Ibid.* **1984**, *3*, 1241.